Optimization for Maximizing Sum Secrecy Rate in MU-MISO SWIPT Systems

Mahmoud Alageli, Aissa Ikhlef, *Member, IEEE*, and Jonathon Chambers, *Fellow, IEEE*

Abstract—In this paper, we consider the sum secrecy rate maximization problem in multiuser multiple-input single-output (MU-MISO) systems in the presence of multiple energy harvesters (EHs) which also have potential to wire-tap the information users (IUs). To facilitate delivering secure information to the IUs and increase the total harvested energy by the EHs simultaneously, we optimise the transmit beamforming vectors to direct the information signals toward the IUs and artificial noise (AN) toward the EHs. We assume that each EH relies on itself to decode the information signal intended for an individual IU. Therefore, the corresponding problem is to maximize the worst-case sum secrecy rate under transmit power and energy harvesting constraints. The problem is optimally solved by transforming it into a convex iterative program using a change of variables, semi-definite relaxation (SDR) and linearization of quadratic terms. We prove that rank-one optimal solutions for the IUs beamforming covariance matrices can be obtained from the optimal relaxed unconstrained solution. Also, we provide three sub-optimal solutions based on null space projection and power control of the beamforming vectors for the low and high harvested energy constrained regions. A special case of cooperative EHs in which the EHs can collaboratively cancel the signal of all IUs except the one they intend to eavesdrop is also investigated, and the optimal solution is derived in a comparable way as in non-cooperative EHs case. Our simulation results reveal an understanding of how the trade-off between the AN and information signal can jointly improve both the sum secrecy rate and the total harvested energy. We also show that, within the low total harvested energy region, the sub-optimal solution in which the AN is projected in the null space of the IUs channels outperforms the sub-optimal solution which ignores AN alignment at the IUs, and vice versa over the high total harvested energy region; and that the suboptimal solution that combines both of them achieves close to optimal performance.

Index Terms—SWIPT, multiuser multi-input single-output (MU-MISO), physical-layer security, sum secrecy rate, energy harvesting, beamforming, artificial noise

I. INTRODUCTION

Recently, the technologies for extending the lifetime of energy constrained wireless networks such as wireless sensor networks have acquired much interest. Wireless power transfer (WPT) is a reliable method for powering remote wireless nodes. The concept of WPT was first introduced by Tesla a century ago [1], since then, a large number of studies have been conducted on WPT for short and medium distances which are mainly based on inductive and magnetic resonance coupling techniques [2]–[4]. However, having tightly coupled aligned devices at short proximity seems to be unattainable in practice. One of the latest promising technologies is that based on utilizing the radio frequency (RF) transmission for simultaneous wireless information and power transfer (SWIPT). A growing body of research has recognised the importance of employing SWIPT technology for multiuser multi-input single-output (MU-MISO) systems [5]–[15] in which there are some users interested in information decoding (IUs) while others wish to perform energy harvesting (EHs). Due to the nature of the broadcast channel and the common practice that the EHs are assumed to be in close proximity to the transmitting antennas compared to the IUs, the implementation of SWIPT faces a security challenge in canceling the crosstalk between IUs and EHs.

The earliest information protection approaches in MISO/MIMO wireless network were typically information-theoretic based such as cryptography techniques attained by applying encryption at the upper protocol layer [16]. The robustness of cryptography techniques relies on the computational hardness required to recover the encryption key, however, such security techniques are not protected against the advances in quantum computing [17]. Although some research works have considered exploiting the reciprocity and randomness of the channel between the transmitter and the IU for secrecy key generation [18]–[21], extra resources are required to secure a wireless channel to share the encryption key between the transmitter at the base station (BS) and the IU, and this is quite difficult in SWIPT with the presence of multiple IUs and EHs which can potentially play the role of eavesdropper.

Latterly, physical layer security (PHY-security) has proven to be a promising alternative to the information-theoretic security techniques. It exploits the knowledge of the transmit channel to provide a better signal quality at the IUs compared to that at the EHs using signal beamforming and jamming techniques. In transmit beamforming, the transmitted signal is precoded in order to strengthen the information signal power at the IUs and to direct artificial noise (AN) toward the EHs. Previous works [7]–[10] have considered the maximization of downlink secrecy rate under certain harvested energy constraints, or as a by-product, the minimization of transmit power under some secrecy rate constraints. For example, the authors in [8] considered a system comprising a single-

M. Alageli and J. Chambers are with the Intelligent Sensing and Communications Group, Newcastle University, NE1 7RU, UK. (e-mail: {m.m.a.alageli1, jonathon.chambers}@ncl.ac.uk). J. Chambers is also with the College of Automation, Harbin Engineering University, China.

A. Ikhlef is with the School of Engineering and Computing Sciences, Durham University, Durham, DH1 3LE, UK. (e-mail: aissa.ikhlef@durham.ac.uk).

antenna IU and multiple single-antenna EHs which collude to cooperatively decode the information signal of the IU. The objective was to optimize the information and the AN beamforming vectors to maximize the secrecy rate subject to individual harvested energy constraints, or to minimize the total transmit power subject to secrecy rate and energy harvesting constraints. The work in [9] assumed that each IU employs a power splitting approach to decode information and harvest energy simultaneously and each user is cooperatively wire-taped by the remaining IUs. The considered problem was to minimize the total transmit power under constraints on individual harvested energy and secrecy rate. In [10], the problem was to maximize the minimum secrecy rate of an IU and EH pair under constraints on minimum individual harvested energy by the IUs and EHs. EHs are passive which means they can either harvest energy or decode information at a time, whereas the IUs employ power splitting for SWIPT. Cooperative jamming techniques have also been considered for PHY-security [12]–[15]. In [12], the secrecy rate of the intended user was improved by employing a cooperative jammer (CJ) which generates AN toward a single eavesdropper to assist in degrading its information signal quality and supply the EH and IU with wireless power. The problem of maximizing the secrecy rate for the worst-case channel uncertainties and under transmit power constraints and EH constraints was decoupled into three problems and solved alternately.

SWIPT has also been considered for the frequency selective environment [22]–[25]. The authors in [22] used orthogonal frequency division multiplexing access (OFDMA) to address the maximization of the harvested energy of a single eavesdropper while maintaining the minimum individual secrecy rate requirements of legitimate users by alternately optimizing subcarrier allocation and power splitting ratio at the legitimate users.

In the earlier works [6], [8], the authors considered similar system models to the multiple IUs model considered in this paper, but for a single IU and multiple EHs in [6] and for a single IU and colluding eavesdroppers in [8]. The objective function for secrecy rate maximization in [6] was a difference between two logarithms of linear fractional functions which correspond to the IU's information rate and the information rate at the worst EH. The problem was solved by one-dimensional search through a set of optimised IU's signal-to-noise ratios (SNRs) which correspond to a set of common upper bound constraints on the SNR at the EHs. The linear fractional objective function was convexified by semi-definite relaxation (SDR) and the Charnes-Cooper transformation. The same methods were applied in [8] but for colluding eavesdroppers and imperfect channel state information (CSI). However, considering multiple IUs (for sum secrecy rate maximization) will result in a non-linear fractional objective function which inevitably can not be optimally solved by the method for a single IU used in [6] due to the non-linearity of the fractional objective function, and this leads to a completely different optimization challenge. Another issue of considering multiple IUs compared to a single IU model in [6] is that the dimensionality of the null space of the IUs channel matrix decreases as the number of IUs increases, i.e., the column size

of $\text{null}(\boldsymbol{H}) \in \mathbb{C}^{N \times N - M}$ decreases as M increases, where $\boldsymbol{H}$ is the channel matrix of the IUs and M is the number of IUs. Therefore, any further beamforming using $\text{null}(\boldsymbol{H})$ will lose the gain of M coefficients.

In this work, an MISO SWIPT system comprising multiple IUs and multiple EHs is considered. We employ transmit beamforming for the information signal and the AN to maximize the worst-case sum secrecy rate of the IUs and the sum secrecy rate for the case of cooperative EHs with a lower limit on the total harvested energy by the EHs (the problem with individual harvested energy constraints has also been considered). To the best of the authors' knowledge, this problem has not been considered in the literature before. More precisely, we provide optimal solutions based on a semidefinite programming (SDP) formulation. Using dual multipliers which satisfy Slater's condition [26] and the Karush-Kuhn-Tucker (KKT) conditions of the SDP problem, we derive a rank-one optimal solution which achieves the same objective value as the optimal rank-unconstrained solution. In addition, we provide two different sub-optimal solutions for the low and high harvested energy constraint regions based on null space projection (NSP) of the beamforming vectors with per beamforming vector power control. By employing both AN beamforming vectors (optimized by different sub-optimal solutions), we tackle the gain loss due to dimensionality reduction of the null space of the IUs channel matrix and a close to optimal performance is achieved.

The remainder of the paper is organized as follows. Section II introduces the system model and Section III presents the original formulation of the sum secrecy rate maximization problem for the non-cooperative EHs case. In Section IV, we provide the optimal solution for the non-cooperative EHs case. Sub-optimal solutions for the non-cooperative EHs case are provided in Section V. In Section VI, a special case of non-cooperative EHs is presented and in Section VII we provide the complexity analysis of the proposed solutions. Numerical results and evaluations are presented in Section VIII. Finally, conclusions are given in Section IX.

Notation: Vectors are denoted by boldface lower case letters and matrices by boldface upper case letters. $\boldsymbol{I}_N$, $\boldsymbol{0}_{m \times n}$ and $\boldsymbol{1}_M$ denote an $N \times N$ identity matrix, an $m \times n$ zero matrix and an $M \times 1$ column vector with all entries one, respectively. $\text{diag}(\boldsymbol{x})$ denotes a diagonal matrix with the elements of $\boldsymbol{x}$ in the main diagonal. $Re(\boldsymbol{Q})$ and $Im(\boldsymbol{Q})$ denote the real and imaginary parts of matrix $\boldsymbol{Q}$, respectively. $\boldsymbol{S} \succeq 0$ indicates that $\boldsymbol{S}$ is a positive semi-definite matrix. $\mathbb{R}$ denotes the set of real numbers. The operators $(\cdot)^T$, $(\cdot)^H$, $\text{Tr}(\cdot)$, $\log(\cdot)$, $\log_2(\cdot)$, $|\cdot|$ and $\|\cdot\|_F$ denote the transpose, conjugate transpose, trace of a matrix, natural logarithm, logarithm to base 2, absolute value of scalars and Frobenius norm of matrices, respectively. $\|[x_1, ..., x_M]\|_1 = \sum_{i=1}^{M} |x_i|$. $\mathbb{C}^{m \times n}$ denotes the set of all complex $m \times n$ matrices. $\boldsymbol{x} \sim \mathcal{CN}(\boldsymbol{0}, \boldsymbol{\Sigma})$ denotes a circularly symmetric complex Gaussian random vector $\boldsymbol{x} \in \mathbb{C}^{N \times 1}$ with zero mean and covariance matrix $\boldsymbol{\Sigma}$. $\{\boldsymbol{a}_n\}$ denotes a set of all vectors indexed by n. $[\boldsymbol{a}]_i$, $\dim(\boldsymbol{a})$ denote the ith entry and the length of the vector $\boldsymbol{a}$, respectively. $\boldsymbol{x} \succeq 0$ means that $[\boldsymbol{x}]_i \geq 0$, $i = 1, ..., \dim(\boldsymbol{x})$. $\boldsymbol{B} = \text{null}(\boldsymbol{A})$, which means, $\boldsymbol{AB} = 0$ and $\boldsymbol{BB}^H = I$.
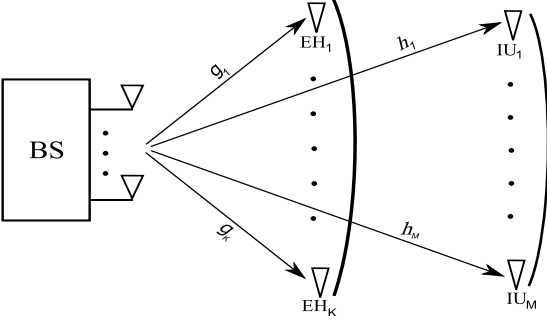
Fig. 1. An MU-MISO SWIPT system comprising multiple IUs and multiple EHs.

II. SYSTEM MODEL

Consider a flat fading single-cell MU-MISO downlink system as shown in Fig. 1. The system comprises a base station (BS) with N antennas, $M < N$ single-antenna IUs, $\{IU_i\}$, $i = 1, ..., M$, interested in information decoding and K single-antenna EHs, $\{EH_k\}$, $k = 1, ..., K$, wishing to perform energy harvesting. The EHs are assumed to be located closer to the BS compared to the IUs in order to harvest energy from the BS transmitted RF signal. Let $\boldsymbol{H} = [\boldsymbol{h}_1, ..., \boldsymbol{h}_M]^H \in \mathbb{C}^{M \times N}$ and $\boldsymbol{G} = [\boldsymbol{g}_1, ..., \boldsymbol{g}_K]^H \in \mathbb{C}^{K \times N}$ be the channel matrices between the BS and IUs, EHs, respectively, with $\boldsymbol{h}_i \sim \mathcal{CN}\left(\boldsymbol{0}, \gamma_I^2 \boldsymbol{I}_N\right)$, $\boldsymbol{g}_k \sim \mathcal{CN}\left(\boldsymbol{0}, \gamma_E^2 \boldsymbol{I}_N\right)$. The BS is assumed to have full knowledge of $\boldsymbol{H}$ and $\boldsymbol{G}$. To facilitate secure information transmission, the BS employs transmit beamforming to steer M information signal beams toward the IUs along with $L \leq N$ AN beams directed toward the EHs to degrade their received information signal quality. Let $\boldsymbol{x} = [x_1, ..., x_M]^T$, $\boldsymbol{W} = [\boldsymbol{w}_1, ..., \boldsymbol{w}_M] \in \mathbb{C}^{N \times M}$ and $\boldsymbol{Q} = [\boldsymbol{q}_1, ..., \boldsymbol{q}_L] \in \mathbb{C}^{N \times L}$ denote the information symbol vector intended for the IUs with $E\left\{\boldsymbol{x}\boldsymbol{x}^H\right\} = \boldsymbol{I}_M$, the information beamforming matrix and the AN beamforming matrix, respectively. The signal received at IU_i, $i = 1, ..., M$, is

$$y_{I_i} = \boldsymbol{h}_i^H \boldsymbol{w}_i x_i + \sum_{\substack{m=1 \\ m \neq i}}^{M} \boldsymbol{h}_i^H \boldsymbol{w}_m x_m + \sum_{l=1}^{L} \boldsymbol{h}_i^H \boldsymbol{q}_l z_l + n_{I_i}, \quad (1)$$

where $n_{I_i} \sim \mathcal{CN}\left(0, \sigma_I^2\right)$ is the noise at IU_i and z_l is the AN symbol. The signal received at EH_k is

$$y_{E_k} = \boldsymbol{g}_k^H \boldsymbol{w}_i x_i + \sum_{\substack{m=1 \\ m \neq i}}^{M} \boldsymbol{g}_k^H \boldsymbol{w}_m x_m + \sum_{l=1}^{L} \boldsymbol{g}_k^H \boldsymbol{q}_l z_l + n_{E_k}, \quad (2)$$

where $n_{E_k} \sim \mathcal{CN}\left(0, \sigma_E^2\right)$ is the noise at EH_k.

In this paper, unless otherwise stated, we assume that each EH relies on itself to decode the information signal intended for the IU_i, i.e., there is no cooperation between the EHs to decode the information signal. According to (1) and (2), with the assumption that the EHs are decoding the information signal without an attempt to harvest energy, the signal-to-interference-plus-noise ratio (SINR) at IU_i, SINR_{I_i}, and the SINR at EH_k intending to wire-tap the IU_i's signal, $\text{SINR}_{E_k}^i$,

are obtained as

$$\text{SINR}_{I_i} = \frac{\left|\boldsymbol{h}_i^H \boldsymbol{w}_i\right|^2}{\sum_{\substack{m=1 \\ m \neq i}}^{M} \left|\boldsymbol{h}_i^H \boldsymbol{w}_m\right|^2 + \sum_{l=1}^{L} \left|\boldsymbol{h}_i^H \boldsymbol{q}_l\right|^2 + \sigma_I^2}, \quad (3)$$

$$\text{SINR}_{E_k}^i = \frac{\left|\boldsymbol{g}_k^H \boldsymbol{w}_i\right|^2}{\sum_{l=1}^{L} \left|\boldsymbol{g}_k^H \boldsymbol{q}_l\right|^2 + \sum_{\substack{m=1 \\ m \neq i}}^{M} \left|\boldsymbol{g}_k^H \boldsymbol{w}_m\right|^2 + \sigma_E^2}. \quad (4)$$

The achievable secrecy rate for IU_i when wire-tapped by EH_k ($R_{i,k}$) is given by

$$R_{i,k} = \max\left(\log_2\left(1 + \text{SINR}_{I_i}\right) - \log_2\left(1 + \text{SINR}_{E_k}^i\right), 0\right). \quad (5)$$

In our system, all EHs can harvest energy from the information and AN signals (we assume that the harvested energy from the noise is negligible). Assuming unit time slot duration and all EHs have the same energy harvesting efficiency $0 \leq \zeta \leq 1$, the total energy harvested by all EHs is

$$E = \zeta \text{Tr}\left(\hat{\boldsymbol{G}}\left(\hat{\boldsymbol{Q}} + \sum_{i=1}^{M} \hat{\boldsymbol{W}}_i\right)\right), \quad (6)$$

where $\hat{\boldsymbol{W}}_i = \boldsymbol{w}_i \boldsymbol{w}_i^H$, $\hat{\boldsymbol{Q}} = \sum_{l=1}^{L} \boldsymbol{q}_l \boldsymbol{q}_l^H$, and $\hat{\boldsymbol{G}} = \boldsymbol{G}^H \boldsymbol{G}$.

III. PROBLEM FORMULATION

Our focus is on optimizing the downlink beamforming matrices for both information and AN signals to maximize the sum secrecy rate of the IUs under given constraints on the minimum total harvested energy received by the EHs and total BS's transmit power P_t. The design aims to maximize the worst-case sum secrecy rate, given by

$$R = \sum_{i=1}^{M} \min_{k} R_{i,k} = \log_2\left(\prod_{i=1}^{M}\left(1 + \text{SINR}_{I_i}\right)\right) - \log_2\left(\prod_{i=1}^{M} \max_{k}\left(1 + \text{SINR}_{E_k}^i\right)\right). \quad (7)$$

Therefore, by expressing the quadratic terms (vector and matrix norms) in terms of linear functions of positive semidefinite matrix variables $\hat{\boldsymbol{W}}_i$, $\hat{\boldsymbol{Q}}$, and deterministic matrices $\boldsymbol{H}_i = \boldsymbol{h}_i \boldsymbol{h}_i^H$, $\boldsymbol{G}_k = \boldsymbol{g}_k \boldsymbol{g}_k^H$ and $\hat{\boldsymbol{G}}$, the SDP optimization problem can be formulated as

$$\underset{\{\hat{\boldsymbol{W}}_i\}, \hat{\boldsymbol{Q}}}{\text{maximize}}$$

$$\log_2\left(\prod_{i=1}^{M} \frac{\sum_{m=1}^{M} \text{Tr}\left(\boldsymbol{H}_i \hat{\boldsymbol{W}}_m\right) + \text{Tr}\left(\boldsymbol{H}_i \hat{\boldsymbol{Q}}\right) + \sigma_I^2}{\sum_{\substack{m=1 \\ m \neq i}}^{M} \text{Tr}\left(\boldsymbol{H}_i \hat{\boldsymbol{W}}_m\right) + \text{Tr}\left(\boldsymbol{H}_i \hat{\boldsymbol{Q}}\right) + \sigma_I^2}\right) -$$

$$\log_2\left(\prod_{i=1}^{M} \max_{k} \frac{\sum_{m=1}^{M} \text{Tr}\left(\boldsymbol{G}_k \hat{\boldsymbol{W}}_m\right) + \text{Tr}\left(\boldsymbol{G}_k \hat{\boldsymbol{Q}}\right) + \sigma_E^2}{\sum_{\substack{m=1 \\ m \neq i}}^{M} \text{Tr}\left(\boldsymbol{G}_k \hat{\boldsymbol{W}}_m\right) + \text{Tr}\left(\boldsymbol{G}_k \hat{\boldsymbol{Q}}\right) + \sigma_E^2}\right)$$

$$\text{subject to} \quad \text{Tr}\left(\hat{\boldsymbol{Q}}\right) + \text{Tr}\left(\sum_{i=1}^{M} \hat{\boldsymbol{W}}_i\right) \leq P_t, \quad (8a)$$

$$\zeta \operatorname{Tr}\left(\hat{\boldsymbol{G}}\left(\hat{\boldsymbol{Q}} + \sum_{i=1}^{M} \hat{\boldsymbol{W}}_i\right)\right) \geq \bar{E}, \qquad (8b)$$

$$\hat{\boldsymbol{W}}_i, \hat{\boldsymbol{Q}} \succeq \boldsymbol{0}, \ \forall i, \qquad (8c)$$

where $\bar{E}$ is the constraint on the total harvested energy by all EHs. It can be seen that the problem has a complicated non-convex objective function which includes logarithms of the product of fractional quadratic functions. The beamforming matrices $\left\{\hat{\boldsymbol{W}}_i\right\}$ should aim to solve a contradicting balance between the following: increasing the information signal power at the IUs, cancelling inter-user interference, reducing the information signal power at the EHs and assisting the EHs to harvest energy. On the other hand, the AN beamforming matrix, $\hat{\boldsymbol{Q}}$, should be optimized to jam the EHs and provide them with a source to harvest energy along with reducing the AN power at the IUs. Since the power budget at the BS is limited, the power allocation between $\operatorname{Tr}\left(\sum_{i=1}^{M} \hat{\boldsymbol{W}}_i\right)$ and $\operatorname{Tr}\left(\hat{\boldsymbol{Q}}\right)$ should be held in the optimal balance. In the following, we provide optimal and suboptimal solutions for the design problems.

IV. OPTIMAL SOLUTION

A. Problem Feasibility and Reformulation

In this section, we solve optimization problem (8) optimally through reformulating the objective function and the non-convex constraints by using a change of variables, linearisation and semidefinite relaxation of quadratic terms. First, let us examine the feasibility of problem (8) through solving the constraints (8a) and (8b). The upper bound of total harvested energy (the largest total energy that could be harvested) is obtained sharply when the BS transmits with its full power, P_t, along with aligning the direction of $\left(\hat{\boldsymbol{Q}} + \sum_{i=1}^{M} \hat{\boldsymbol{W}}_i\right)$ such that

$$\left(\hat{\boldsymbol{Q}} + \sum_{i=1}^{M} \hat{\boldsymbol{W}}_i\right) = P_t \boldsymbol{\varrho}\boldsymbol{\varrho}^H, \qquad (9)$$

where $\boldsymbol{\varrho}$ is the eigenvector which corresponds to the largest eigenvalue of the matrix $\hat{\boldsymbol{G}}$, λ_g [27]. This is the case in which problem (8) is reduced to an energy harvesting maximization problem with information beamforming vectors set to zero, i.e., $\sum_{i=1}^{M} \hat{\boldsymbol{W}}_i = \boldsymbol{0}$, and the BS transmits AN precoded with a single beamforming vector $\boldsymbol{q_1} = \sqrt{P_t}\boldsymbol{\varrho}$. According to this, we can write constraint (8b) as

$$\zeta P_t \lambda_g \geq \zeta \operatorname{Tr}\left(\hat{\boldsymbol{G}}\left(\hat{\boldsymbol{Q}} + \sum_{i=1}^{M} \hat{\boldsymbol{W}}_i\right)\right) \geq \bar{E}. \qquad (10)$$

With the existence of P_t in the left-hand side of (10), the satisfaction of (11) will definitely result in satisfying the constraint (8a), therefore, the feasibility of problem (8) is guaranteed under the following condition

$$\zeta P_t \lambda_g \geq \bar{E}. \qquad (11)$$

Now, let us reformulate the objective function which comprises a product of fractional terms. For this goal, we build upon the change of variable idea proposed in [28]. Let us substitute the numerators and denominators of the fractions in the objective function in (8) by exponential variables as follows

$$e^{u_i} = \sum_{m=1}^{M} \operatorname{Tr}\left(\boldsymbol{H}_i \hat{\boldsymbol{W}}_m\right) + \operatorname{Tr}\left(\boldsymbol{H}_i \hat{\boldsymbol{Q}}\right) + \sigma_I^2, \quad \forall i, \quad (12a)$$

$$e^{s_i} = \sum_{\substack{m=1 \\ m \neq i}}^{M} \operatorname{Tr}\left(\boldsymbol{H}_i \hat{\boldsymbol{W}}_m\right) + \operatorname{Tr}\left(\boldsymbol{H}_i \hat{\boldsymbol{Q}}\right) + \sigma_I^2, \quad \forall i, \quad (12b)$$

$$e^{v_k} = \sum_{m=1}^{M} \operatorname{Tr}\left(\boldsymbol{G}_k \hat{\boldsymbol{W}}_m\right) + \operatorname{Tr}\left(\boldsymbol{G}_k \hat{\boldsymbol{Q}}\right) + \sigma_E^2, \quad \forall k, \quad (12c)$$

$$e^{t_{i,k}} = \sum_{\substack{m=1 \\ m \neq i}}^{M} \operatorname{Tr}\left(\boldsymbol{G}_k \hat{\boldsymbol{W}}_m\right) + \operatorname{Tr}\left(\boldsymbol{G}_k \hat{\boldsymbol{Q}}\right) + \sigma_E^2, \quad \forall i, \ \forall k. \qquad (12d)$$

By using properties of the exponential and the logarithmic functions, we can write the objective function in (8) as $\sum_{i=1}^{M} \left(u_i - s_i - \max_k \left(v_k - t_{i,k}\right)\right)$ whilst constraining u_i, s_i, v_k and $t_{i,k}$ by the expressions at the right hand sides of (12a), (12b), (12c) and (12d), respectively. Therefore, by defining real-valued slack variables $\boldsymbol{u} = [u_1, ..., u_M]^T$, $\boldsymbol{s} = [s_1, ..., s_M]^T$, $\boldsymbol{v} = [v_1, ..., v_K]^T$, $\boldsymbol{T} = \begin{bmatrix} t_{1,1} & \cdots & t_{1,K} \\ \vdots & \ddots & \vdots \\ t_{M,1} & \cdots & t_{M,K} \end{bmatrix}$ and the set of optimization variables $\left\{\left\{\hat{\boldsymbol{W}}_m\right\}, \hat{\boldsymbol{Q}}, \boldsymbol{s}, \boldsymbol{T}, \boldsymbol{u}, \boldsymbol{v}\right\} = \mathbb{S}$, $m = 1, ..., M$, the SDP reformulation of problem (8) is

$$\underset{\mathbb{S}}{\text{maximize}} \quad \sum_{i=1}^{M} \left(u_i - s_i - \max_{k=1,...,K} \left(v_k - t_{i,k}\right)\right)$$

subject to

$$\sum_{m=1}^{M} \operatorname{Tr}\left(\boldsymbol{H}_i \hat{\boldsymbol{W}}_m\right) + \operatorname{Tr}\left(\boldsymbol{H}_i \hat{\boldsymbol{Q}}\right) + \sigma_I^2 \geq e^{u_i}, \ \forall i, \qquad (13a)$$

$$\sum_{\substack{m=1 \\ m \neq i}}^{M} \operatorname{Tr}\left(\boldsymbol{H}_i \hat{\boldsymbol{W}}_m\right) + \operatorname{Tr}\left(\boldsymbol{H}_i \hat{\boldsymbol{Q}}\right) + \sigma_I^2 \leq e^{s_i}, \ \forall i, \qquad (13b)$$

$$\sum_{m=1}^{M} \operatorname{Tr}\left(\boldsymbol{G}_k \hat{\boldsymbol{W}}_m\right) + \operatorname{Tr}\left(\boldsymbol{G}_k \hat{\boldsymbol{Q}}\right) + \sigma_E^2 \leq e^{v_k}, \ \forall k, \qquad (13c)$$

$$\sum_{\substack{m=1 \\ m \neq i}}^{M} \operatorname{Tr}\left(\boldsymbol{G}_k \hat{\boldsymbol{W}}_m\right) + \operatorname{Tr}\left(\boldsymbol{G}_k \hat{\boldsymbol{Q}}\right) + \sigma_E^2 \geq e^{t_{i,k}}, \ \forall t_{i,k}, \qquad (13d)$$

$$\text{(8a), (8b), (8c).} \qquad (13e)$$

The objective function in (13) consists of a sum of affine functions $\left(\sum_{i=1}^{M} u_i - s_i\right)$ minus a sum of maxima of affine functions $\left(\sum_{i=1}^{M} \max_k \left(v_k - t_{i,k}\right)\right)$ which is convex. Therefore, the affine part minus the convex part will result in a concave objective function. To deal with the non-convex constraints (13b) and (13c), we linearize the exponential terms e^{s_i} and e^{v_k} using the first order Taylor approximation, such that $e^{s_i} = e^{\bar{s}_i}\left(s_i - \bar{s}_i + 1\right)$ and $e^{v_k} = e^{\bar{v}_k}\left(v_k - \bar{v}_k + 1\right)$, $\forall i$, where $\bar{\boldsymbol{s}} = [\bar{s}_1, ..., \bar{s}_M]^T$ and $\bar{\boldsymbol{v}}^{(1)} = [\bar{v}_1^{(1)}, ..., \bar{v}_K^{(1)}]^T$

are the points around which the linearizations are made. Also, we drop the rank-one constraint on $\left\{\hat{\boldsymbol{W}}_m\right\}$ such that $\operatorname{rank}\left(\hat{\boldsymbol{W}}_m\right) \leq N, \quad m = 1, ..., M$. Therefore, problem (13) can be recast as

$$\underset{\mathbb{S}}{\text{maximize}} \quad \sum_{i=1}^M \left(u_i - s_i - \max_{k=1,...,K} (v_k - t_{i,k})\right)$$

subject to

$$\sum_{\substack{m=1 \\ m \neq i}}^M \operatorname{Tr}\left(\boldsymbol{H}_i \hat{\boldsymbol{W}}_m\right) + \operatorname{Tr}\left(\boldsymbol{H}_i \hat{\boldsymbol{Q}}\right) + \sigma_I^2$$
$$\leq e^{\bar{s}_i}\left(s_i - \bar{s}_i + 1\right), \ \forall i, \tag{14a}$$

$$\sum_{i=1}^M \operatorname{Tr}\left(\boldsymbol{G}_k \hat{\boldsymbol{W}}_i\right) + \operatorname{Tr}\left(\boldsymbol{G}_k \hat{\boldsymbol{Q}}\right) + \sigma_E^2$$
$$\leq e^{\bar{v}_k}\left(v_k - \bar{v}_k + 1\right), \ \forall k, \tag{14b}$$

$$(13a), (13d), (8a), (8b), (8c). \tag{14c}$$

Problem (14) can be solved iteratively by Algorithm 1 using the CVX optimization software [29].

Algorithm 1 Algorithm for solving problem (14)

1: Initialize $\bar{\boldsymbol{s}}^{[j]}$ and $\bar{\boldsymbol{v}}^{[j]}$, $j = 1$.
2: **Repeat**
3: Solve problem (14) and calculate $\left\{\hat{\boldsymbol{W}}_i\right\}^{[j]}, \hat{\boldsymbol{Q}}^{[j]}, \boldsymbol{s}^{[j]}, \boldsymbol{v}^{[j]}$.
4: Increment $j = j + 1$.
5: Update the initial values $\bar{\boldsymbol{s}}^{[j]} = \boldsymbol{s}^{[j-1]}$ and $\bar{\boldsymbol{v}}^{[j]} = \boldsymbol{v}^{[j-1]}$.
6: **Until** Convergence.
7: Calculate $\boldsymbol{W}$ and $\boldsymbol{Q}$ from $\left\{\hat{\boldsymbol{W}}_i\right\}$ and $\hat{\boldsymbol{Q}}$.

Remark 1: To guarantee sufficient harvested energy for all EHs, problem (14) can be recast by replacing the total harvested energy constraint (8b) with individual energy harvesting constraints as

$$\underset{\mathbb{S}}{\text{maximize}} \quad \sum_{i=1}^M \left(u_i - s_i - \max_{k=1,...,K} (v_k - t_{i,k})\right)$$

subject to

$$\zeta \operatorname{Tr}\left(\boldsymbol{G}_k \left(\hat{\boldsymbol{Q}} + \sum_{i=1}^M \hat{\boldsymbol{W}}_i\right)\right) \geq \hat{E}, \ \forall k, \tag{15a}$$

$$(14a), (14b), (13a), (13d), (8a), (8c). \tag{15b}$$

where $\hat{E}$ is the minimum harvested energy per individual EH.

B. Optimal Rank-one Solution to the SDR Reformulation

In the solutions $\left\{\hat{\boldsymbol{W}}_m^{\star_1}\right\}$ and $\left\{\hat{\boldsymbol{W}}_m^{\star_2}\right\}$, $m = 1, ..., M$, obtained by solving problems (14) and (15), respectively, there is no guarantee that $\operatorname{rank}\left(\hat{\boldsymbol{W}}_m^{\star_j}\right) = 1$, $j = 1, 2, \forall m$, such that it can take the form $\hat{\boldsymbol{W}}_m^{\star_j} = \boldsymbol{w}_m^{\star_j} \boldsymbol{w}_m^{\star_j H}$. Therefore, if $\operatorname{rank}\left(\hat{\boldsymbol{W}}_m^{\star_j}\right) = 1$, then the optimal beamforming vectors are calculated using eigenvalue decomposition. Otherwise, if $\operatorname{rank}\left(\hat{\boldsymbol{W}}_m^{\star_j}\right) > 1$, building upon the framework in [6], [7], an optimal rank-one solution can be calculated by using the following theorem.

Theorem 1: Having the optimal solutions $\left\{\left\{\hat{\boldsymbol{W}}_m^{\star_j}\right\}, \hat{\boldsymbol{Q}}^{\star_j}, \boldsymbol{s}^{\star_j}, \boldsymbol{T}^{\star_j}, \boldsymbol{u}^{\star_j}, \boldsymbol{v}^{\star_j}\right\} = \mathbb{S}^{\star_j}$, $j = 1, 2$, for SDR problems (14) and (15), respectively, with $\operatorname{rank}\left(\hat{\boldsymbol{W}}_{\bar{m}}^{\star_j}\right) > 1$, $\{\bar{m}\} \subset \{1, ..., M\}$ and $\{\bar{m}\} \neq \phi$. Then, there exist optimal solutions $\left\{\left\{\widetilde{\boldsymbol{W}}_m^{\star_j}\right\}, \widetilde{\boldsymbol{Q}}^{\star_j}, \widetilde{\boldsymbol{s}}^{\star_j}, \widetilde{\boldsymbol{T}}^{\star_j}, \boldsymbol{u}^{\star_j}, \boldsymbol{v}^{\star_j}\right\} = \widetilde{\mathbb{S}}^{\star_j}$, $j = 1, 2$, for the SDR problems (14) and (15), respectively, that satisfy a rank-one constraint, $\operatorname{rank}\left(\widetilde{\boldsymbol{W}}_{\bar{m}}^{\star_j}\right) = 1$ and can achieve the same objective value achieved by $\mathbb{S}^{\star_j}$, $j = 1, 2$, respectively.

Proof: See the Appendix. ∎

V. Suboptimal Solutions

In this subsection, we derive suboptimal solutions to problem (8) with lower complexity. The solution is based on designing the directions of $\boldsymbol{w}_i$s to nullify the information signal interference whilst maximizing the information signal for each information user. In addition, two different beamforming vectors for the AN are considered, $\boldsymbol{q}_1$ and $\boldsymbol{q}_2$. The vector $\boldsymbol{q}_1$ is designed to nullify the AN at the IUs while $\boldsymbol{q}_2$ ignores AN alignment at the IUs. The direction design is followed by per beamformer power control.

Let $\tilde{\boldsymbol{H}}_i = [\boldsymbol{h}_1, ..., \boldsymbol{h}_{i-1}, \boldsymbol{h}_{i+1}, \boldsymbol{h}_M]^H$ with a singular value decomposition (SVD) $\tilde{\boldsymbol{H}}_i = \boldsymbol{U}_i \boldsymbol{\Sigma}_i \left[\boldsymbol{V}_i \bar{\boldsymbol{V}}_i\right]^H$, where $\bar{\boldsymbol{V}}_i \in \mathbb{C}^{N \times (N-M+1)}$ contains the last $N - M + 1$ right-singular vectors with $\bar{\boldsymbol{V}}_i^H \bar{\boldsymbol{V}}_i = \boldsymbol{I}_{N-M+1}$. The vectors constituting $\bar{\boldsymbol{V}}_i$ are the basis for the right null space of $\tilde{\boldsymbol{H}}_i$, i.e., $\tilde{\boldsymbol{H}}_i \bar{\boldsymbol{V}}_i = \boldsymbol{0}_{(M-1) \times (N-M+1)}$. Therefore, to nullify the information signal interference at the IU$_i$, we should design the IU$_i$'s beamformer as

$$\boldsymbol{w}_i = \sqrt{p_i}\bar{\boldsymbol{w}}_i = \sqrt{p_i}\bar{\boldsymbol{V}}_i \hat{\boldsymbol{w}}_i, \tag{16}$$

where p_i is the power assigned to $\boldsymbol{w}_i$ and $\hat{\boldsymbol{w}}_i \in \mathbb{C}^{(N-M+1) \times 1}$ is an arbitrary unit norm complex vector. To maximize the signal at the IU$_i$, $\hat{\boldsymbol{w}}_i$ is aligned to the direction of the equivalent channel $\boldsymbol{h}_i^H \bar{\boldsymbol{V}}_i$, i.e., $\hat{\boldsymbol{w}}_i = \frac{\bar{\boldsymbol{V}}_i^H \boldsymbol{h}_i}{\left|\bar{\boldsymbol{V}}_i^H \boldsymbol{h}_i\right|}$.

Using a similar concept, we design the direction of the AN beamforming vector, $\boldsymbol{q}_1$. Let $\boldsymbol{H} = \boldsymbol{U} \boldsymbol{\Sigma} \left[\boldsymbol{V}\bar{\boldsymbol{V}}\right]^H$ be the singular value decomposition of $\boldsymbol{H}$, with $\bar{\boldsymbol{V}} \in \mathbb{C}^{N \times (N-M)}$ containing the last $N - M$ right-singular vectors. Therefore, it can be guaranteed that there is no AN leakage to the IUs, i.e., $\boldsymbol{H}\boldsymbol{q}_1 = \boldsymbol{0}_{M \times 1}$, by designing $\boldsymbol{q}_1$ as

$$\boldsymbol{q}_1 = \sqrt{p_{n_1}}\bar{\boldsymbol{q}}_1 = \sqrt{p_{n_1}}\bar{\boldsymbol{V}}\hat{\boldsymbol{q}}_1, \tag{17}$$

where p_{n_1} is the AN power of $\boldsymbol{q}_1$ and $\hat{\boldsymbol{q}}_1 \in \mathbb{C}^{(N-M) \times 1}$ is an arbitrary complex unit norm vector. The total power harvested by the EHs from the AN is $p_{n_1} \left\|\boldsymbol{G}\bar{\boldsymbol{V}}\hat{\boldsymbol{q}}_1\right\|_F^2$. Let $\boldsymbol{\nu}$ be the unit norm eigenvector corresponding to the largest eigenvalue value of the matrix $\bar{\boldsymbol{V}}^H \boldsymbol{G}^H \boldsymbol{G}\bar{\boldsymbol{V}}$, then, to maximize the total harvested energy, the optimal value of $\hat{\boldsymbol{q}}_1$ is $\hat{\boldsymbol{q}}_1 = \boldsymbol{\nu}$. The other AN beamforming vector, $\boldsymbol{q}_2$, aims to maximize the total harvested energy without paying attention to the noise it imposes on the IUs. Therefore

$$\boldsymbol{q}_2 = \sqrt{p_{n_2}}\bar{\boldsymbol{q}}_2, \tag{18}$$

where p_{n_2} is the AN power of $\boldsymbol{q}_2$, $\bar{\boldsymbol{q}}_2$ is the unit norm eigenvector corresponding to the largest eigenvalue value of the matrix $\boldsymbol{G}^H\boldsymbol{G}$.

Now, we establish three sub-optimal solutions based on three different sets of AN beamforming vectors; the first sub-optimal solution, sub(1), uses the AN beamforming vector $\mathbb{Q}_1 = \{\bar{\boldsymbol{q}}_1\}$, the second sub-optimal solution, sub(2), uses the AN beamforming vector $\mathbb{Q}_2 = \{\bar{\boldsymbol{q}}_2\}$, while the third sub-optimal solution, sub(3), uses two AN beamforming vectors $\mathbb{Q}_3 = \{\bar{\boldsymbol{q}}_1, \bar{\boldsymbol{q}}_2\}$. Based on the designed directions of $\{\boldsymbol{w}_i\}$, we write the secrecy rate for IU$_i$, when wire-tapped by EH$_k$ and using the $\mathbb{Q}_j$, $j = 1, 2, 3$, set of AN beamforming vectors, as

$$
R_{i,k}^{\text{sub}(j)} = \log_2\left(\frac{p_i\left|\boldsymbol{h}_i^H\bar{\boldsymbol{w}}_i\right|^2 + p_{n_2}\left|\boldsymbol{h}_i^H\bar{\boldsymbol{q}}_2\right|^2 + \sigma_I^2}{p_{n_2}\left|\boldsymbol{h}_i^H\bar{\boldsymbol{q}}_2\right|^2 + \sigma_I^2}\right) -
$$
$$
\max_k \log_2\left(\frac{\sum_{i=1}^M p_i\left|\boldsymbol{g}_k^H\bar{\boldsymbol{w}}_i\right|^2 + \sum_{l\in\mathbb{I}_j} p_{n_l}\left|\boldsymbol{g}_k^H\bar{\boldsymbol{q}}_l\right|^2 + \sigma_E^2}{\sum_{\substack{m=1\\m\neq i}}^M p_m\left|\boldsymbol{g}_k^H\bar{\boldsymbol{w}}_m\right|^2 + \sum_{l\in\mathbb{I}_j} p_{n_l}\left|\boldsymbol{g}_k^H\bar{\boldsymbol{q}}_l\right|^2 + \sigma_E^2}\right),
$$
$$
\tag{19}
$$

where $\mathbb{I}_1$, $\mathbb{I}_2$ and $\mathbb{I}_3$ are index sets containing the indices of the vectors in $\mathbb{Q}_1$, $\mathbb{Q}_2$ and $\mathbb{Q}_3$, respectively. Now, we define three different problems P(j), $j = 1, 2, 3$, corresponding to the use of the three different sets of AN beamforming vectors $\mathbb{Q}_1$, $\mathbb{Q}_2$ and $\mathbb{Q}_3$. The power vector $\boldsymbol{P} = [p_1, ..., p_M]$ and p_{n_1}, p_{n_2}, are optimized to maximize the worst-case sum secrecy rate $\left(R^{\text{sub}(j)} = \sum_{i=1}^M \min_k R_{i,k}^{\text{sub}(j)}\right)$ by solving the following problem P(j) (change of variables and Taylor approximation are exploited to formulate the problem)

$$
\text{P}(j): \underset{\substack{\hat{\boldsymbol{u}},\hat{\boldsymbol{s}},\hat{\boldsymbol{v}},\hat{\boldsymbol{T}},\\\boldsymbol{P},p_{n_1},p_{n_2}}}{\text{maximize}} \sum_{i=1}^M\left(\hat{u}_i - \hat{s}_i - \max_k\left(\hat{v}_k - \hat{t}_{i,k}\right)\right)
$$

subject to

$$
p_i\left|\boldsymbol{h}_i^H\bar{\boldsymbol{w}}_i\right|^2 + p_{n_2}\left|\boldsymbol{h}_i^H\bar{\boldsymbol{q}}_2\right|^2 + \sigma_I^2 \geq e^{\hat{u}_i}, \ \forall i, \tag{20a}
$$

$$
p_{n_2}\left|\boldsymbol{h}_i^H\bar{\boldsymbol{q}}_2\right|^2 + \sigma_I^2 \leq e^{\bar{\hat{s}}_i}\left(\hat{s}_i - \bar{\hat{s}}_i + 1\right), \ \forall i, \tag{20b}
$$

$$
\sum_{i=1}^M p_i\left|\boldsymbol{g}_k^H\bar{\boldsymbol{w}}_i\right|^2 + \sum_{l\in\mathbb{I}_j} p_{n_l}\left|\boldsymbol{g}_k^H\bar{\boldsymbol{q}}_l\right|^2 + \sigma_E^2 \leq
$$
$$
e^{\bar{\hat{v}}_k}\left(\hat{v}_k - \bar{\hat{v}}_k + 1\right), \ \forall k, \tag{20c}
$$

$$
\sum_{\substack{m=1\\m\neq i}}^M p_m\left|\boldsymbol{g}_k^H\bar{\boldsymbol{w}}_m\right|^2 + \sum_{l\in\mathbb{I}_j} p_{n_l}\left|\boldsymbol{g}_k^H\bar{\boldsymbol{q}}_l\right|^2 + \sigma_E^2 \geq e^{\hat{t}_{i,k}}, \forall\hat{t}_{i,k},
$$
$$
\tag{20d}
$$

$$
\sum_{l\in\mathbb{I}_j} p_{n_l} + \sum_{i=1}^M p_i \leq P_t, \tag{20e}
$$

$$
\sum_{i=1}^M p_i\left\|\boldsymbol{G}\bar{\boldsymbol{w}}_i\right\|_F^2 + \sum_{l\in\mathbb{I}_j} p_{n_l}\left\|\boldsymbol{G}\bar{\boldsymbol{q}}_l\right\|_F^2 \geq \bar{E}, \tag{20f}
$$

where $\hat{\boldsymbol{u}} = [\hat{u}_1, ..., \hat{u}_M]^T$, $\hat{\boldsymbol{s}} = [\hat{s}_1, ..., \hat{s}_M]^T$, $\hat{\boldsymbol{v}} = [\hat{v}_1, ..., \hat{v}_K]^T$ and $\hat{\boldsymbol{T}} = \begin{bmatrix} \hat{t}_{1,1} & ... & \hat{t}_{1,K} \\ \vdots & \ddots & \vdots \\ \hat{t}_{M,1} & ... & \hat{t}_{M,K} \end{bmatrix}$ are slack variables. Problem (20) is solved iteratively, after each iteration, $\bar{\hat{\boldsymbol{s}}} = [\bar{\hat{s}}_1, ..., \bar{\hat{s}}_M]^T$ and $\bar{\hat{\boldsymbol{v}}} = [\bar{\hat{v}}_1, ..., \bar{\hat{v}}_K]^T$, the Taylor initial value in (20b) and (20c), are updated by the optimized value of $\hat{\boldsymbol{s}}$ and $\hat{\boldsymbol{v}}$. The iterations continue until convergence in a similar manner to that in Algorithm 1.

Remark 2: To guarantee sufficient harvested energy for all EHs, problem (20) can be recast by replacing the total harvested energy constraint (20f) with individual energy harvesting constraints as

$$
\bar{\text{P}}(j): \underset{\substack{\hat{\boldsymbol{u}},\hat{\boldsymbol{s}},\hat{\boldsymbol{v}},\hat{\boldsymbol{T}},\\\boldsymbol{P},p_{n_1},p_{n_2}}}{\text{maximize}} \sum_{i=1}^M\left(\hat{u}_i - \hat{s}_i - \max_k\left(\hat{v}_k - \hat{t}_{i,k}\right)\right)
$$

subject to

$$
\sum_{i=1}^M p_i\left|\boldsymbol{g}_k^H\bar{\boldsymbol{w}}_i\right|_F^2 + \sum_{l\in\mathbb{I}_j} p_{n_l}\left|\boldsymbol{g}_k^H\bar{\boldsymbol{q}}_l\right|_F^2 \geq \hat{E}, \ \forall k \tag{21a}
$$

$$
(20a), (20b), (20c), (20d), (20e). \tag{21b}
$$

Problem (21) can be solved iteratively in a similar manner as in (20).

VI. SPECIAL CASE OF COOPERATIVE EHs

In this section, we consider a special case when all EHs cooperate to decode the IU$_i$'s signal, therefore, they have the ability to cancel the information signal interference. The sum secrecy rate in this case is given by

$$
\log_2\left(\prod_{i=1}^M \frac{\sum_{m=1}^M \text{Tr}\left(\boldsymbol{H}_i\hat{\boldsymbol{W}}_m\right) + \text{Tr}\left(\boldsymbol{H}_i\hat{\boldsymbol{Q}}\right) + \sigma_I^2}{\sum_{\substack{m=1\\m\neq i}}^M \text{Tr}\left(\boldsymbol{H}_i\hat{\boldsymbol{W}}_m\right) + \text{Tr}\left(\boldsymbol{H}_i\hat{\boldsymbol{Q}}\right) + \sigma_I^2}\right.
$$
$$
\left.\times \frac{\text{Tr}\left(\hat{\boldsymbol{G}}\hat{\boldsymbol{Q}}\right) + K\sigma_E^2}{\text{Tr}\left(\hat{\boldsymbol{G}}\hat{\boldsymbol{W}}_i\right) + \text{Tr}\left(\hat{\boldsymbol{G}}\hat{\boldsymbol{Q}}\right) + K\sigma_E^2}\right). \tag{22}
$$

Defining real-valued slack variables $\ddot{v}$ and $\ddot{\boldsymbol{t}} = [\ddot{t}_1, ..., \ddot{t}_M]^T$ and the set of optimization variables $\left\{\boldsymbol{u}, \boldsymbol{s}, \ddot{v}, \ddot{\boldsymbol{t}}, \left\{\hat{\boldsymbol{W}}_m\right\}, \hat{\boldsymbol{Q}}\right\} = \ddot{\mathbb{S}}$, $m = 1, ..., M$, the SDP reformulation of the sum secrecy rate maximization problem is

$$
\underset{\ddot{\mathbb{S}}}{\text{maximize}} \sum_{i=1}^M\left(u_i - s_i + \ddot{v} - \ddot{t}_i\right)
$$

subject to

$$
\text{Tr}\left(\hat{\boldsymbol{G}}\hat{\boldsymbol{Q}}\right) + K\sigma_E^2 \geq e^{\ddot{v}}, \tag{23a}
$$

$$
\text{Tr}\left(\hat{\boldsymbol{G}}\hat{\boldsymbol{W}}_i\right) + \text{Tr}\left(\hat{\boldsymbol{G}}\hat{\boldsymbol{Q}}\right) + K\sigma_E^2 \leq e^{\bar{\ddot{t}}_i}\left(\ddot{t}_i - \bar{\ddot{t}}_i + 1\right), \ \forall i, \tag{23b}
$$

$$
(13a), (14a), (13e). \tag{23c}
$$

Problem (23) is solved iteratively, after each iteration, $\bar{\ddot{\boldsymbol{t}}} = [\bar{\ddot{t}}_1, ..., \bar{\ddot{t}}_M]^T$ and $\bar{\boldsymbol{s}}$ (see constraint (14a)) are updated by

the optimized value of $\ddot{\boldsymbol{t}}$ and $\boldsymbol{s}$. The iterations continue until convergence in a similar manner to that in Algorithm 1.

By following comparable steps as in the proof of *Theorem I*, given the optimal rank-unconstrained solution of problem (23), $\ddot{\mathbb{S}}^\star = \left\{ \left\{ \hat{\boldsymbol{W}}_m^\star \right\}, \hat{\boldsymbol{Q}}^\star, \boldsymbol{s}^\star, \ddot{\boldsymbol{t}}^\star, \boldsymbol{u}^\star, \ddot{v}^\star \right\}$, we can calculate an optimal solution $\widetilde{\mathbb{S}} = \left\{ \left\{ \widetilde{\boldsymbol{W}}_m \right\}, \widetilde{\boldsymbol{Q}}, \widetilde{\boldsymbol{s}}, \ddot{\boldsymbol{t}}^\star, \boldsymbol{u}^\star, \widetilde{v} \right\}$ that satisfies the rank-one constraints, $\operatorname{rank}\left(\widetilde{\boldsymbol{W}}_{\bar{m}} \right) = 1$, $\bar{m} \in \left\{ m : \operatorname{rank}\left(\hat{\boldsymbol{W}}_m^\star \right) > 1 \right\}$ and achieves the same objective value as $\ddot{\mathbb{S}}^\star$ does, as follows

$$
\widetilde{\boldsymbol{W}}_m = \bar{b}_{m,\bar{n}_{1_m}} \bar{\boldsymbol{\omega}}_{m,\bar{n}_m} \bar{\boldsymbol{\omega}}_{m,\bar{n}_m}^H = \begin{cases} \hat{\boldsymbol{W}}_m^\star - \bar{\boldsymbol{\tau}}_m & \forall m \in \{\bar{m}\} \\ \hat{\boldsymbol{W}}_m^\star, & \forall m \notin \{\bar{m}\} \end{cases},
\tag{24}
$$

$$
\widetilde{s}_m =
\begin{cases}
s_m^\star + \bar{\delta}_m^{(1)}, & \forall m \in \{\bar{m}\}, \sum\limits_{\bar{m}} \operatorname{Tr}\left(\boldsymbol{H}_{\bar{m}} \bar{\boldsymbol{\tau}}_{\bar{m}} \right) \le \operatorname{Tr}\left(\hat{\boldsymbol{G}} \sum\limits_{\bar{m}} \bar{\boldsymbol{\tau}}_m \right) \\
s_m^\star + \bar{\delta}_m^{(2)}, & \forall m \in \{\bar{m}\}, \sum\limits_{\bar{m}} \operatorname{Tr}\left(\boldsymbol{H}_{\bar{m}} \bar{\boldsymbol{\tau}}_{\bar{m}} \right) \ge \operatorname{Tr}\left(\hat{\boldsymbol{G}} \sum\limits_{\bar{m}} \bar{\boldsymbol{\tau}}_m \right) \\
s_m^\star, & \forall m \notin \{\bar{m}\}
\end{cases}
\tag{25}
$$

$$
\widetilde{v} =
\begin{cases}
\ddot{v}^\star + \sum\limits_{\bar{m}} \bar{\delta}_m^{(1)}, & \forall m \in \{\bar{m}\}, \sum\limits_{\bar{m}} \operatorname{Tr}\left(\boldsymbol{H}_{\bar{m}} \bar{\boldsymbol{\tau}}_{\bar{m}} \right) \le \operatorname{Tr}\left(\hat{\boldsymbol{G}} \sum\limits_{\bar{m}} \bar{\boldsymbol{\tau}}_m \right) \\
\ddot{v}^\star + \sum\limits_{\bar{m}} \bar{\delta}_m^{(2)}, & \forall m \in \{\bar{m}\}, \sum\limits_{\bar{m}} \operatorname{Tr}\left(\boldsymbol{H}_{\bar{m}} \bar{\boldsymbol{\tau}}_{\bar{m}} \right) \ge \operatorname{Tr}\left(\hat{\boldsymbol{G}} \sum\limits_{\bar{m}} \bar{\boldsymbol{\tau}}_m \right) \\
\ddot{v}^\star, & \forall m \notin \{\bar{m}\}
\end{cases}
\tag{26}
$$

$$
\widetilde{\boldsymbol{Q}} = \hat{\boldsymbol{Q}}^\star + \sum_{m \in \{\bar{m}\}} \bar{\boldsymbol{\tau}}_m,
\tag{27}
$$

where

$$
\bar{n}_m \in \{1, ..., \bar{r}_{2_m} - \bar{r}_{1_m}\},
\tag{28}
$$

$$
\bar{\boldsymbol{\tau}}_m = \sum_{n=1}^{N-\bar{r}_{2_m}} \bar{a}_{m,n} \bar{\boldsymbol{\psi}}_{m,n} \bar{\boldsymbol{\psi}}_{m,n}^H + \sum_{\substack{n_1=1 \\ n_1 \ne \bar{n}_{1_m}}}^{N-\bar{r}_m} \bar{b}_{m,n_1} \bar{\boldsymbol{\omega}}_{m,n_1} \bar{\boldsymbol{\omega}}_{m,n_1}^H,
\tag{29}
$$

$$
\bar{\delta}_m^{(1)} = -s_m^\star + \log\left(\operatorname{Tr}\left(\boldsymbol{H}_m \bar{\boldsymbol{\tau}}_m \right) + e^{s_m^\star} \right),
\tag{30}
$$

$$
\bar{\delta}_m^{(2)} = -\ddot{v}^\star + \log\left(\frac{\operatorname{Tr}\left(\boldsymbol{H}_m \bar{\boldsymbol{\tau}}_m \right)}{\sum\limits_{\bar{m}} \operatorname{Tr}\left(\boldsymbol{H}_m \bar{\boldsymbol{\tau}}_m \right)} \sum\limits_{\bar{m}} \operatorname{Tr}\left(\hat{\boldsymbol{G}} \boldsymbol{\tau}_m \right) + e^{\ddot{v}^\star} \right),
\tag{31}
$$

$$
\bar{r}_{1_m} = \operatorname{rank}\left(\ddot{\boldsymbol{Y}}_m^\star \right), \qquad \bar{r}_{2_m} = \operatorname{rank}\left(\ddot{\boldsymbol{D}}_m^\star \right),
\tag{32}
$$

$$
\left[\bar{\boldsymbol{\psi}}_{m,1}, ..., \bar{\boldsymbol{\psi}}_{m,N-\bar{r}_{2_m}} \right] = \bar{\boldsymbol{\Psi}}_m = \operatorname{null}\left(\ddot{\boldsymbol{D}}_m^\star \right),
\tag{33}
$$

$$
\left[\bar{\boldsymbol{\Psi}}_m \left[\bar{\boldsymbol{\omega}}_{m,1}, ..., \bar{\boldsymbol{\omega}}_{m,\bar{r}_{2_m}-\bar{r}_{1_m}} \right] \right] = \operatorname{null}\left(\ddot{\boldsymbol{Y}}_m^\star \right),
\tag{34}
$$

$$
\ddot{\boldsymbol{Y}}_m^\star = \ddot{\boldsymbol{D}}_m^\star - \sum_{i=1}^{M} \beta_{3_i}^\star \boldsymbol{H}_i, \qquad \ddot{\boldsymbol{D}}_m^\star = \beta_1^\star - \zeta \beta_2^\star \hat{\boldsymbol{G}},
\tag{35}
$$

and $\beta_1^\star$, $\beta_2^\star$, $\left\{ \beta_{3_i}^\star \right\}$, $\left\{ \ddot{\boldsymbol{Y}}_m^\star \right\}$, are the optimal multipliers associated with the constraints (8a), (8b), (13a) and the positive semidefinitness constraints of $\left\{ \hat{\boldsymbol{W}}_m \right\}$ in (8c), respectively; $\bar{a}_{m,n}$s > 0 and $\bar{b}_{m,n_1}$s > 0 are positive scaling constants.

By using the beamforming vectors $\boldsymbol{w}_i$s, $\boldsymbol{q}_1$ and $\boldsymbol{q}_2$ in (16)-(18), and defining new slack variables $\check{v}$ and $\check{\boldsymbol{t}} = \left[\check{t}_1, ..., \check{t}_M \right]^T$, three different suboptimal solutions for sum secrecy rate maximization can be obtained by formulating problems having a similar structure to problem (20) as follows

$$
\hat{\mathrm{P}}(j): \operatorname*{maximize}_{\hat{\boldsymbol{u}}, \hat{\boldsymbol{s}}, \check{v}, \check{\boldsymbol{t}}, \boldsymbol{P}, p_{n_1}, p_{n_2}} \sum_{i=1}^{M} \left(\hat{u}_i - \hat{s}_i + \check{v} - \check{t}_i \right)
$$

subject to

$$
p_i \| \boldsymbol{G}\bar{\boldsymbol{w}}_i \|_F^2 + \sum_{l \in \mathbb{I}_j} p_{n_l} \| \boldsymbol{G}\bar{\boldsymbol{q}}_l \|_F^2 + K\sigma_E^2 \le
$$
$$
e^{\check{t}_i} \left(\check{t}_i - \bar{\check{t}}_i + 1 \right), \ \forall i,
\tag{36a}
$$

$$
\sum_{l \in \mathbb{I}_j} p_{n_l} \| \boldsymbol{G}\bar{\boldsymbol{q}}_l \|_F^2 + K\sigma_E^2 \ge e^{\check{v}},
\tag{36b}
$$

$$
(20a), (20b), (20e), (20f).
\tag{36c}
$$

Problem (36) is solved iteratively, after each iteration, $\bar{\check{\boldsymbol{t}}} = \left[\bar{\check{t}}_1, ..., \bar{\check{t}}_M \right]^T$ and $\bar{\hat{\boldsymbol{s}}}$ (see constraint (20b)) are updated by the optimized value of $\check{\boldsymbol{t}}$ and $\hat{\boldsymbol{s}}$, respectively. The iterations continue until convergence in a similar manner to that in Algorithm 1.

VII. Complexity Analysis

The complexity of our solutions (the optimal and the sub optimal) relate to the type of the optimization problems, the size of input data, number of the required iterations and the methods used to solve them. The most generic problems, (14) for the optimal solution and $P(3)$ in (20) for the suboptimal solution are convex and solved by CVX software. The solvers used by CVX software (such as SDPT3 and SeDuMi) employ a symmetric primal-dual interior-point algorithm which cannot handle the exponential function in the constraints (13a), (13d), (20a) and (20d). Therefore, CVX uses the successive approximation method in which the exponential functions are approximated in a polynomial form, and then the resulting problem is solved iteratively until convergence [29]–[31]. The per-iteration problem for the formulation in (14) is equivalent to an SDP problem, while, the per-iteration problem for $P(3)$ in (20) is equivalent to a linear program (LP). For similar convergence tolerance, we compare the complexity of both problems, (14) and $P(3)$ in (20) by comparing the complexity of the per-iteration problems. For that purpose, we use the basic complexity analysis steps in chapter 6 in [32].

A. Complexity of Suboptimal Solution

To follow the steps of the complexity analysis given in chapter 6 in [32], we need to transform the per-iteration problem for $P(3)$ in (20) (in which all exponential functions are approximated by first order polynomials) into an equivalent standard LP form. First, we transform the max operator expression

in the objective function $\left(\sum_{i=1}^{M} \max_{k=1,...,K}\left(\hat{v}_k - \hat{t}_{i,k}\right)\right)$ by introducing a new vector slack variable $\boldsymbol{\pi} \in \mathbb{R}^{M \times 1}$ such that the max operator expression will be $\mathbf{1}_M^T \boldsymbol{\pi}$, where $\mathbf{1}_M$ is a $M \times 1$ vector with all entries one, with KM constraints (per scalar value) $[\boldsymbol{\pi}]_i \geq \hat{v}_k - [\boldsymbol{t}_k]_i$, $\forall i$, $\forall k$, where $\boldsymbol{t}_k \in \mathbb{R}^{M \times 1}$ is the kth column of $\hat{\boldsymbol{T}}$. Now we can transform the per-iteration problem in its standard LP form as follows

$$(P_{\text{sub}}): \underset{\boldsymbol{x}}{\text{maximize}} \quad \boldsymbol{c}^T \boldsymbol{x}$$

$$\text{subject to}$$

$$\boldsymbol{A}_{(1)}\,\boldsymbol{x} \ \succeq \ \boldsymbol{d}_1, \tag{37a}$$
$$\boldsymbol{A}_{(2)}\,\boldsymbol{x} \ \preceq \ \boldsymbol{d}_2, \tag{37b}$$
$$\boldsymbol{A}_{(3)}\,\boldsymbol{x} \ \preceq \ \boldsymbol{d}_3, \tag{37c}$$
$$\boldsymbol{A}_{(4_k)}\,\boldsymbol{x} \ \succeq \ \boldsymbol{d}_{4_k}, \quad \forall k, \tag{37d}$$
$$\boldsymbol{a}_{(5)}^T\,\boldsymbol{x} \ \leq \ P_t, \tag{37e}$$
$$\boldsymbol{a}_{(6)}^T\,\boldsymbol{x} \ \geq \ \bar{E}, \tag{37f}$$
$$\boldsymbol{A}_{(7_k)}\,\boldsymbol{x} \ \succeq \ \boldsymbol{0}, \quad \forall k, \tag{37g}$$
$$\boldsymbol{A}_{(8)}\,\boldsymbol{x} \ \succeq \ \boldsymbol{0}. \tag{37h}$$

where

$\boldsymbol{x} = \left[p_1,...,p_M, p_{n_1}, p_{n_2}, \hat{\boldsymbol{u}}^T, \hat{\boldsymbol{s}}^T, \hat{\boldsymbol{v}}^T, \boldsymbol{t}_1^T,...,\boldsymbol{t}_K^T, \boldsymbol{\pi}^T\right]^T$, $\boldsymbol{c} = \left[\boldsymbol{0}_{1 \times M+2}, \mathbf{1}_M^T, -\mathbf{1}_M^T, \boldsymbol{0}_{1 \times (M+1)K}, \mathbf{1}_M^T\right]^T$, $\boldsymbol{A}_{(1)} = \left[\boldsymbol{a}_{(1_1)}^T,...,\boldsymbol{a}_{(1_M)}^T\right]$, $\boldsymbol{A}_{(2)} = \left[\boldsymbol{a}_{(2_1)}^T,...,\boldsymbol{a}_{(2_M)}^T\right]$, $\boldsymbol{A}_{(3)} = \left[\boldsymbol{a}_{(3_1)}^T,...,\boldsymbol{a}_{(3_K)}^T\right]$, $\boldsymbol{A}_{(4_k)} = \left[\boldsymbol{a}_{(4_{k1})}^T,...,\boldsymbol{a}_{(4_{kM})}^T\right]$, $\boldsymbol{a}_{(5)} = \left[\mathbf{1}_{M+2}^T, \boldsymbol{0}_{1 \times (3+K)M+K}\right]^T$, $\boldsymbol{A}_{(7_k)} = \left[\boldsymbol{a}_{(7_{k1})}^T,...,\boldsymbol{a}_{(7_{kM})}^T\right]$, $\boldsymbol{a}_{(7_{ki})} = \left[\boldsymbol{0}_{1 \times 3M+2+k-1}, -1, \boldsymbol{0}_{1 \times K-k+(k-1)M+i-1}, 1, \boldsymbol{0}_{1 \times (K-k+1)M-1}, 1, \boldsymbol{0}_{1 \times M-i}\right]^T$, $\boldsymbol{A}_{(8)} = \left[\boldsymbol{I}_{M+2}, \boldsymbol{0}_{M+2 \times (3+K)M+K}\right]^T$, $[\boldsymbol{d}_1]_i = -\sigma_I^2 + e^{\hat{u}_i}\left(1 - \hat{u}_i\right)$, $[\boldsymbol{d}_2]_i = -\sigma_I^2 + e^{\hat{s}_i}\left(1 - \hat{s}_i\right)$, $[\boldsymbol{d}_3]_k = -\sigma_E^2 + e^{\hat{v}_k}\left(1 - \hat{v}_k\right)$, $[\boldsymbol{d}_{4_k}]_i = -\sigma_E^2 + e^{\hat{t}_{i,k}}\left(1 - \hat{t}_{i,k}\right)$, and — $\hat{u}_i$, $\hat{s}_i$, $\forall i$, $\hat{v}_k$, $\forall k$ and $\hat{t}_{i,k}$, $\forall i$ $\forall k$ are the initial values of first order approximation,

$$[\boldsymbol{a}_{(1_i)}]_j = \begin{cases} \left|\boldsymbol{h}_i^H \bar{\boldsymbol{w}}_i\right|^2, & j = i \\ \left|\boldsymbol{h}_i^H \bar{\boldsymbol{q}}_2\right|^2, & j = M+2 \\ -e^{\hat{u}_i}, & j = M+2+i \\ 0, & \text{otherwise} \end{cases} \tag{38}$$

$$[\boldsymbol{a}_{(2_i)}]_j = \begin{cases} \left|\boldsymbol{h}_i^H \bar{\boldsymbol{q}}_2\right|^2, & j = M+2 \\ -e^{\hat{s}_i}, & j = 2M+2+i \\ 0, & \text{otherwise} \end{cases} \tag{39}$$

$$[\boldsymbol{a}_{(3_k)}]_j = \begin{cases} \left|\boldsymbol{g}_k^H \bar{\boldsymbol{w}}_j\right|^2, & j = 1,...,M \\ \left|\boldsymbol{g}_k^H \bar{\boldsymbol{q}}_j\right|^2, & j = M+1, M+2 \\ -e^{\hat{v}_k}, & j = 3M+2+k \\ 0, & \text{otherwise} \end{cases} \tag{40}$$

$$[\boldsymbol{a}_{(6)}]_j = \begin{cases} \|\boldsymbol{G}\bar{\boldsymbol{w}}_j\|_F^2, & j = 1,...,M \\ \|\boldsymbol{G}\bar{\boldsymbol{q}}_j\|_F^2, & j = M+1, M+2 \\ 0, & \text{otherwise} \end{cases} \tag{41}$$

$$[\boldsymbol{a}_{(4_{ki})}]_j = \begin{cases} \left|\boldsymbol{g}_k^H \bar{\boldsymbol{w}}_j\right|^2, & j = 1,...,i-1,i+1,...,M \\ \left|\boldsymbol{g}_k^H \bar{\boldsymbol{q}}_j\right|^2, & j = M+1, M+2 \\ -e^{\hat{t}_{i,k}}, & j = 3M+K+2+M(i-1)+k \\ 0, & \text{otherwise} \end{cases} \tag{42}$$

With the standard LP formulation in (37), the complexity of attaining an optimized objective value within an accuracy ϵ, $\text{Comp}\left(P_{\text{sub}}, \epsilon\right)$, is calculated in terms of the following parameters:

$n_s = \dim \boldsymbol{x} = (4+K)M + K + 2$, the dimension of real design variables; $m_s = (3+2K)M + K + 4$, the total number of per-scalar value constraints; and $\text{Data}\left(P_{\text{sub}}\right) = \left[n_s, m_s, \boldsymbol{c}^T, \text{vec}\left(\boldsymbol{A}_{(1)}\right)^T, \text{vec}\left(\boldsymbol{A}_{(2)}\right)^T, \text{vec}\left(\boldsymbol{A}_{(3)}\right)^T, \text{vec}\left(\boldsymbol{A}_{(4_1)}\right)^T,..., \text{vec}\left(\boldsymbol{A}_{(4_K)}\right)^T, \boldsymbol{a}_{(5)}^T, \boldsymbol{a}_{(6)}^T, \text{vec}\left(\boldsymbol{A}_{(7_1)}\right)^T,..., \text{vec}\left(\boldsymbol{A}_{(7_K)}\right)^T, \text{vec}\left(\boldsymbol{A}_{(8)}\right)^T, \boldsymbol{d}_1^T, \boldsymbol{d}_2^T, \boldsymbol{d}_3^T, \boldsymbol{d}_{4_1}^T,..., \boldsymbol{d}_{4_K}^T, P_t, \bar{E}\right]^T$, input data vector for P_{sub} where $\dim \text{Data}\left(P_{\text{sub}}\right) = (3n_s + 2n_s K + K + 2)M + (n_s+1)K + 4n_s + 4$.

The per-iteration complexity in terms of the number of real operations, $\text{Comp}\left(P_{sub}, \epsilon\right)$, is calculated as [32]

$$\text{Comp}\left(P_{\text{sub}}, \epsilon\right) = (n_s + m_s)^{\frac{3}{2}}\, n_s^2$$
$$\times \ln\left(\frac{\dim \text{Data}\left(P_{\text{sub}}\right) + \|\text{Data}\left(P_{\text{sub}}\right)\|_1 + \epsilon^2}{\epsilon}\right). \tag{43}$$

The result in (43) assumes that the input data matrices and vectors are unstructured. However, the solver can utilize this matrix structure to reduce the number of operations required for getting the solution.

B. Complexity of Optimal Solution

As in the previous subsection, the first step in analyzing the complexity of the per-iteration problem of (14) is to transform it into a standard SDP form with all constraints expressed in terms of linear matrix inequalities (LMIs). For this purpose, we use the idea of the Schur complement to describe the quadratic constraint in terms of semidefinitness of the bock matrix. For example, the constraint (14a) is transformed into an LMI constraint as described below

$$\boldsymbol{h}_i^H \left(-\hat{\boldsymbol{Q}} - \left(\sum_{\substack{m=1 \\ m \neq i}}^{M} \hat{\boldsymbol{W}}_m\right) + \frac{-\sigma_I^2 + e^{\bar{s}_i}(s_i - \bar{s}_i + 1)}{\|\boldsymbol{h}_i\|^2} \boldsymbol{I}_N\right) \boldsymbol{h}_i$$
$$\leq 0, \ \forall i, \tag{44a}$$

$$\Updownarrow$$

$$\boldsymbol{C}_{1_i} = \begin{bmatrix} \boldsymbol{D}_i^{-1} & \boldsymbol{h}_i \\ \boldsymbol{h}_i^H & 0 \end{bmatrix} =$$
$$\begin{bmatrix} \left(\hat{\boldsymbol{Q}} + \left(\sum_{\substack{m=1 \\ m \neq i}}^{M} \hat{\boldsymbol{W}}_m\right) + \frac{\sigma_I^2 - e^{\bar{s}_i}(s_i - \bar{s}_i + 1)}{\|\boldsymbol{h}_i\|^2} \boldsymbol{I}_N\right)^{-1} & \boldsymbol{h}_i \\ \boldsymbol{h}_i^H & 0 \end{bmatrix}$$
$$\succeq \boldsymbol{0} \quad \forall i. \tag{44b}$$

We get (44a) from (14a) based on properties of the trace operator and matrix multiplication, and the independence between $\left\{\hat{\boldsymbol{W}}_m\right\}$ and $\hat{\boldsymbol{Q}}$. The non-singularity of $\boldsymbol{D}_i$ is guaranteed by

the non-zero identity. The block matrix in (44b) is positive semidefinite if and only if both the lower-right sub-matrix (scalar), 0, and the Schur complement of the upper-left sub-matrix D_i^{-1} in C_{1_i}, $0 - h_i^H D_i^{-1} h_i$, are positive semidefinite. Since the positive semidefinitness of the scalar 0 is always true, therefore the constraints (44b) and (14a) are equivalent. The remaining constraints, (14b), (13a), (13d), (8a) and (8b) are transformed in the same way (after first order linearization of the exponential variables). As in the previous subsection, the max operator expression in the objective function $\left(\sum_{i=1}^M \max_{k=1,\dots,K} \left(v_k - t_{i,k} \right) \right)$ is recast as $\mathbf{1}_M^T \hat{\boldsymbol{\pi}}$, where $\hat{\boldsymbol{\pi}} \in \mathbb{R}^{M \times 1}$ is a vector slack variable, with KM constraints (per scalar value) $[\hat{\boldsymbol{\pi}}]_i \geq v_k - [\boldsymbol{t}_k]_i$, $\forall i$, $\forall k$, where $\boldsymbol{t}_k \in \mathbb{R}^{M \times 1}$ is the kth column of $\boldsymbol{T}$.

Using the fact that the diagonal matrix is positive semidefinite if and only if each of its entries are ≥ 0, the KM constraints $[\hat{\boldsymbol{\pi}}]_i \geq v_k - [\boldsymbol{t}_k]_i$, $\forall i$, $\forall k$, can be transformed to LMI constraints as[1]

$$(\hat{\boldsymbol{\pi}} + \boldsymbol{t}_k - v_k)^T \boldsymbol{I}_M \succeq \mathbf{0} \ \ \forall k. \tag{45}$$

The per-iteration problem for (14) is thereby written in its standard SDP form as follows

$$(P_{\text{opt}}): \ \underset{\boldsymbol{x}}{\text{maximize}} \quad \hat{\boldsymbol{c}}^T \hat{\boldsymbol{x}}$$

$$\text{subject to}$$

$$\boldsymbol{C}_{1_i}, \ \boldsymbol{C}_{2_k}, \ \boldsymbol{C}_{3_i}, \ \boldsymbol{C}_{4_{i,k}} \ \succeq \ \mathbf{0}, \quad \forall i, \ \forall k, \tag{46a}$$

$$\boldsymbol{C}_5, \ \boldsymbol{C}_6 \ \succeq \ \mathbf{0}, \tag{46b}$$

$$\boldsymbol{c}_{7_k} \ \succeq \ \mathbf{0}, \quad \forall k, \tag{46c}$$

$$\hat{\boldsymbol{W}}_i, \hat{\boldsymbol{Q}} \succeq \mathbf{0}. \ \forall i, \tag{46d}$$

where

$$\hat{\boldsymbol{x}} = \left[\boldsymbol{u}^T, \boldsymbol{s}^T, \boldsymbol{v}^T, \hat{\boldsymbol{t}}_1^T, \dots, \hat{\boldsymbol{t}}_K^T, \hat{\boldsymbol{\pi}}^T \right]^T,$$

$$\hat{\boldsymbol{c}} = \left[\mathbf{1}_M^T, -\mathbf{1}_M^T, \mathbf{0}_{1 \times (M+1)K}, \mathbf{1}_M^T \right]^T,$$

$$\boldsymbol{C}_{2_k} =$$
$$\left[\begin{matrix} \left(\hat{\boldsymbol{Q}} + \left(\sum_{m=1}^M \hat{\boldsymbol{W}}_i \right) + \frac{\sigma_E^2 - e^{\bar{v}_k}(v_k - \bar{v}_k + 1)}{\|\boldsymbol{g}_k\|^2} \boldsymbol{I}_N \right)^{-1} & \boldsymbol{g}_k \\ \boldsymbol{g}_k^H & 0 \end{matrix} \right],$$

$$\boldsymbol{C}_{3_i} =$$
$$\left[\begin{matrix} \left(-\hat{\boldsymbol{Q}} - \left(\sum_{m=1}^M \hat{\boldsymbol{W}}_m \right) + \frac{-\sigma_I^2 + e^{\bar{u}_i}(u_i - \bar{u}_i + 1)}{\|\boldsymbol{h}_i\|^2} \boldsymbol{I}_N \right)^{-1} & \boldsymbol{h}_i \\ \boldsymbol{h}_i^H & 0 \end{matrix} \right],$$

$$\boldsymbol{C}_{4_{i,k}} =$$
$$\left[\begin{matrix} \left(-\hat{\boldsymbol{Q}} - \left(\sum_{\substack{m=1 \\ m \neq i}}^M \hat{\boldsymbol{W}}_m \right) - \frac{\sigma_E^2 - e^{\bar{t}_{i,k}}(t_{i,k} - \bar{t}_{i,k} + 1)}{\|\boldsymbol{g}_k\|^2} \boldsymbol{I}_N \right)^{-1} & \boldsymbol{g}_k \\ \boldsymbol{g}_k^H & 0 \end{matrix} \right]$$

$$\boldsymbol{C}_5 = \left[\begin{matrix} \left(\hat{\boldsymbol{Q}} + \left(\sum_{i=1}^M \hat{\boldsymbol{W}}_i \right) - \frac{P_t}{N} \boldsymbol{I}_N \right)^{-1} & \mathbf{1}_N \\ \mathbf{1}_N^H & 0 \end{matrix} \right],$$

$$\boldsymbol{C}_6 =$$

$$\begin{cases} \left[\begin{matrix} \left(-\zeta \left(\hat{\boldsymbol{Q}} + \left(\sum_{i=1}^M \hat{\boldsymbol{W}}_i \right) \right) + \frac{\bar{E}}{N} \boldsymbol{I}_N \right)^{-1} & \mathbf{1}_N \\ \mathbf{1}_N^H & 0 \end{matrix} \right] & , \bar{E} \neq 0, \\ 0 & , \bar{E} = 0 \end{cases}$$

$$\boldsymbol{c}_{7_k} = (\hat{\boldsymbol{\pi}} + \boldsymbol{t}_k - v_k)^T \boldsymbol{I}_M.$$

The standard SDP problem in (46) is represented in a complex-valued domain. Translating the complex-valued domain SDP (CSDP) programme to a real-valued domain SDP programme was introduced in [33] using linear complex-to-real mapping. In our case, we translate the CSDP programme, P_{opt}, to the real-valued domain using the following mapping

$$\mathcal{T}\hat{\boldsymbol{Q}} = \left[\begin{matrix} Re\left(\hat{\boldsymbol{Q}} \right) & -Im\left(\hat{\boldsymbol{Q}} \right) \\ Im\left(\hat{\boldsymbol{Q}} \right) & Re\left(\hat{\boldsymbol{Q}} \right) \end{matrix} \right], \ \mathcal{T}\boldsymbol{g}_k = \left[\begin{matrix} Re\left(\boldsymbol{g}_k \right) \\ Im\left(\boldsymbol{g}_k \right) \end{matrix} \right], \ \forall k,$$

$$\mathcal{T}\hat{\boldsymbol{W}}_i = \left[\begin{matrix} Re\left(\hat{\boldsymbol{W}}_i \right) & -Im\left(\hat{\boldsymbol{W}}_i \right) \\ Im\left(\hat{\boldsymbol{W}}_i \right) & Re\left(\hat{\boldsymbol{W}}_i \right) \end{matrix} \right], \ \mathcal{T}\boldsymbol{h}_i = \left[\begin{matrix} Re\left(\boldsymbol{h}_i \right) \\ Im\left(\boldsymbol{h}_i \right) \end{matrix} \right],$$

$$\forall i, \ \mathcal{T}\mathbf{1}_N = \mathbf{1}_{2N}, \mathcal{T}0 = \mathbf{0}_{2 \times 1} \ \text{in} \ \boldsymbol{C}_5 \ \text{and} \ \boldsymbol{C}_6. \tag{47}$$

Considering the standard SDP formulation (46) in the real-valued domain, we use the method in chapter 6 in [32] to calculate the complexity of attaining an optimized objective value within accuracy ϵ, $\text{Comp}\left(P_{\text{opt}}, \epsilon \right)$, in terms of the following parameters

$n_o = \dim \hat{\boldsymbol{x}} + (M+1)N^2 = (K+3)M + K + 2(M+1)N^2$, the dimension of real design variables; $m_o = KM + 2K + 2M + 4$, the total number of LMI constraints which includes: $(KM + K + M + 3)$ LMI constraints each of size $(2N+2) \times (2N+2)$, K LMI constraints each of size $M \times M$ and $(M+1)$ LMI constraints each of size $N \times N$; $\text{Data}\left(P_{\text{opt}} \right) = \left[n_o, \ m_o, \ \hat{\boldsymbol{c}}^T, \ 4\text{ vec}\left(\boldsymbol{C}_1 \right)^T, \ 4\text{ vec}\left(\boldsymbol{C}_{2_1} \right)^T, \ \dots, \right.$
$4 \text{ vec}\left(\boldsymbol{C}_{2_K} \right)^T, \quad 4 \text{ vec}\left(\boldsymbol{C}_{3_1} \right)^T, \quad \dots, \quad 4 \text{ vec}\left(\boldsymbol{C}_{3_M} \right)^T,$
$4 \text{ vec}\left(\boldsymbol{C}_{4_{1,1}} \right)^T, \quad \dots, \quad 4 \text{ vec}\left(\boldsymbol{C}_{4_{M,K}} \right)^T, \quad 4 \text{ vec}\left(\boldsymbol{C}_5 \right)^T,$
$\left. 4 \text{ vec}\left(\boldsymbol{C}_6 \right)^T \right]$.

The per-iteration complexity in terms of number of real operations, $\text{Comp}\left(P_{\text{opt}}, \epsilon \right)$, is calculated as [32]

$$\text{Comp}\left(P_{\text{opt}}, \epsilon \right) =$$
$$\sqrt{(KM + K + M + 3)(2N+2) + KM + (M+1)N^2}$$
$$n_o \left[n_o^2 + n_o \left((KM + K + M + 3)(2N+2)^2 + KM^2 + \right. \right.$$
$$(M+1)N^2 \right) + (KM + K + M + 3)(2N+2)^3 + KM^3 +$$
$$\left. (M+1)N^3 \right] \ln\left(\frac{\dim \text{Data}\left(P_{\text{opt}} \right) + \|\text{Data}\left(P_{\text{opt}} \right)\|_1 + \epsilon^2}{\epsilon} \right). \tag{48}$$

The solver can benefit from the structure of the LMI matrices in the real-valued domain to reduce the number of real operations. It can be seen that P_{sub} has an $\mathcal{O}\left(K^{\frac{7}{2}} M^{\frac{7}{2}} \left[\ln(K^2 M) + \ln(\frac{1}{\epsilon}) \right] \right)$ asymptotic[1] complexity which is lower than that of the P_{opt}, $\mathcal{O}\left(K^2 M^{\frac{3}{2}} N^8 \left[\ln(N^2 M) + \ln(\frac{1}{\epsilon}) \right] \right)$.

It should be mentioned that, for the suboptimal solution, there is a pre-optimization processing for calculating $\{\bar{\boldsymbol{w}}_i\}$

---

[1] The vector inequality $\boldsymbol{x} \succeq \mathbf{0}$ is equivalent to the LMI $\text{diag}(\boldsymbol{x}) \succeq \mathbf{0}$.

[1] The complexity as $K, M, N \to \infty$, $\epsilon \to 0^+$ and $K \leq N$, $M < N$

and $\{\bar{q}_1, \bar{q}_2\}$, the pre-optimization has an $\mathcal{O}\left(M^3 N\right)$ asymptotic complexity due to the SVD of M matrices of size $(M-1) \times N$. Comparably, for the optimal solution, there is a post-optimization processing for a rank reduction process of $\leq M$ $\hat{\boldsymbol{W}}_i^{\star 1}$s. This post-processing is upper bounded by an $\mathcal{O}\left(MN^3\right)$ asymptotic complexity.

VIII. EVALUATIONS

In this section, we assess the performance of our proposed schemes. The simulation parameters of our MISO SWIPT system includes: number of transmit antennas N, number of single-antenna IUs M, number of single-antenna IUs K, path-loss (variance of the magnitude of channel coefficient) between the transmit antenna, and the receive antenna at the IU and EH, γ_I^2 and γ_E^2, respectively, total transmit power budget available at the BS, P_t, and energy harvesting efficiency ζ.

Parameter selection was made based on some practical models and implementation requirements as follows:

- We set the restrictions $N > M$ and $N \geq K$. Having $N > M$ allows null space generation for the channel matrix between the BS and the IUs, H, i.e., dim null(H) = $N \times (N - M)$ does exist. Consequently, we can project the AN in the null space of H. $N \geq K$ allows the EHs to collude and cancel the interference from non-intended IUs [34]. The selected values are $N = 8$, $M = 2$ and $K = 3$.
- We assume that all IUs are at equal distances from the BS and likewise for the EHs. This assumption is to avoid the selection based on average path-loss which remains static for a long time and focus on the optimization of the beamforming matrices depending upon small-scale fading coefficients.
- For selecting the values of γ_I^2 and γ_E^2 we rely on the general urban channel model $\text{PL}_{\text{dB}} = 10 \log_{10} r^\alpha + b$ [35]. With path-loss coefficient $\alpha = 2$, fixed-loss component $b = 10$ dB which depends on the operating frequency, height of transmit antennas and different macro-environment type. The common assumption is that the EHs are located closer to the BS compared to the IUs in order to harvest energy. We assume that the IUs are located at 1000 m apart from the BS and this corresponds to 70dB path-loss and $\gamma_I^2 = 10^{-7}$, while the EHs are located at 10 m from the BS and this corresponds to 30dB path-loss and $\gamma_E^2 = 10^{-3}$.
- Apart from the design of the energy harvesting circuit, the energy harvesting efficiency mainly varies in accordance with the range of incident RF power. With total transmit power $P_t = 1W$ and 30 dB average path-loss, the incident RF power at the EHs is about 0 dBm which yields an energy harvesting efficiency of at least 50% [36]. Also, the parameter values $P_t = 1$ W and $\zeta = 0.5$ give a decent feasibility region through which system performance can be demonstrated.

We show the system performances in terms of the achievable worst-case sum secrecy rates $\left(R, R^{\text{sub}(1)}, R^{\text{sub}(2)}, R^{\text{sub}(3)}\right)$ against the total harvested energy constraint $\bar{E}$ and individual harvested energy constraint $\hat{E}$. We call the area under the plot (R-E curve) the R-E region and it shows the trade-off between $\bar{E}$ or $\hat{E}$ and the sum secrecy rate. The larger the R-E region the better the performance.

Fig. 2 shows the R-E regions for the non-cooperative EHs case. With regards to the optimal solution, it can be seen that the worst-case sum secrecy rate decreases as the required total harvested energy increases. The trade-off region lies approximately over the total harvested energy constraint interval $(1.5, 7.3]$ mW. This means the power allocated to the AN is zero when $\bar{E} \leq 1.5$ mW, in other words, the energy harvested from the information signal is enough to satisfy this total harvested energy constraint. At the point corresponding to, $\bar{E} = 7.3$ mW, the power allocated to the information signal approaches zero and the problem is being reduced to the energy harvesting maximization problem. On the other hand, the sub-optimal solutions (achieved via LP optimization) have a lower complexity than the optimal solution (achieved via SDP optimization). The sub-optimal solutions' performances lie under the optimal solution. In the sub-optimal solution achieved by the AN beamforming vector $\boldsymbol{q}_1$, Sub(1), there is a gap in the total harvested energy between the optimal and the sub-optimal solution, Δ_E, at zero sum secrecy rate. This gap which is equal to 38% of the optimal total harvested energy ($\frac{\Delta_E}{7.4} \times 100$) is due to the nulling of the AN at the IUs. In other words, in the optimal solution, the AN is matched to all N transmit channels, while in the sub-optimal solution, some degree of freedom of the AN beamforming vector is traded for nullifying the AN at the IUs, therefore, the AN is matched equivalently to only $N - M$ (the column dimension of $G\bar{V}$) channels. This issue of dimensionality reduction appears when serving multiple IUs. The solution Sub(1) performs better over the low total harvested energy constraint region, where the gap between the optimal and the sub-optimal sum secrecy rates, Δ_R, at zero harvested energy constraint is equal to 13% of the optimal sum secrecy rate ($\frac{\Delta_R}{3.85} \times 100$). Conversely, in the sub-optimal solution Sub(2), all N channel coefficients of $\boldsymbol{q}_2$ are matched to the dominant eigenvector of $\boldsymbol{G}^H \boldsymbol{G}$, therefore, the maximum energy is harvested at zero secrecy rate, and the gap in the total harvested energy between the optimal and the sub-optimal solutions totally vanishes. In the sub-optimal solution Sub(3), better performance is achieved by exploiting both AN beamforming vectors $\boldsymbol{q}_1$ and $\boldsymbol{q}_2$, the achievable sum secrecy rate of the sub-optimal solution Sub(3) exploits the advantage of the good performance of Sub(1) and Sub(2) over different regions of $\bar{E}$. It can be seen that $R^{\text{sub}(3)}$ traces the envelope of $R^{\text{sub}(1)}$ and $R^{\text{sub}(2)}$, i.e., $R^{\text{sub}(3)} = \max\left(R^{\text{sub}(1)}, R^{\text{sub}(2)}\right)$.

Fig. 3 shows the E-R region when the EHs cooperate to wire-tap an individual IUs. The same observations in Fig. 2 for the non-cooperative EHs are valid for the cooperative EHs case.

Fig. 4 shows the E-R regions for the non-cooperative EHs case but with individual harvested energy constraints for the optimal and Sub(3) (achieved by solving $\bar{\text{P}}(3)$ in (21)) solutions. The achievable worst-case sum secrecy rate with respect to $\hat{E}$ follows a similar trend to that with respect to $\bar{E}$ given in Fig. 2. By comparing the results in Fig. 4 and Fig. 2, we notice that the achievable worst-case sum secrecy rates corresponding to $\hat{E} = 0$ and $\bar{E} = 0$ are equal since both

problems (14) and (15) are equivalent to a worst-case sum secrecy rate maximization problems with no harvested energy constraints. The Sub(3) solution achieves zero worst-case sum secrecy rates at a value of $\hat{E} = 1.5\ mW$ which is lower than the value of the optimal solution, $\hat{E} = 2.2\ mW$. This is because in the Sub(3) solution the AN beamforming vectors, $\boldsymbol{q}_1$ and $\boldsymbol{q}_2$, are designed to maximize the total harvested energy while the problem is constrained with the individual harvested energy of the EHs.

For the given system parameters and the considered cases, cooperative and non-cooperative EHs represent the worse-case and the best-case assumptions, respectively. The cooperative EHs are equivalent to a single receiver with K receive antenna. Now, with the restriction $K \leq N$, the best scenario for the EHs is to employ successive interference cancellation which is capable of cancelling the interference from non-intended IUs and achieves the best possible information rate [34]. Therefore, the achievable sum secrecy rate can be considered as a lower bound on the optimal solution[1] performance. In the other case, non-cooperative EHs, the assumption is that each EH relies on itself to decode the intended IU signal. In addition, in our objective in (8), we optimize the worst-case sum secrecy rate, i.e., the case when the IU_i are being eavesdropped by the strongest EH_k (see the max operator term in (8)). Therefore, the achievable sum secrecy rate can be considered as an upper bound on the optimal solution performance.
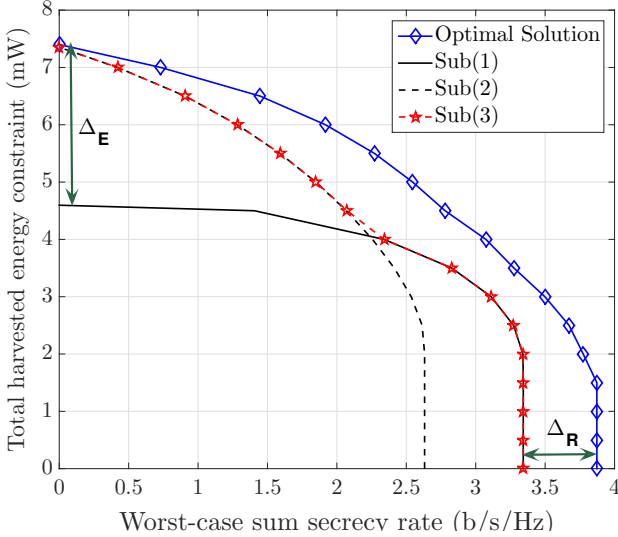

Fig. 2. E-R regions for the non-cooperative EHs case with total harvested energy constraint.

Fig. 5 shows the effect of the placement of the IUs and the non-cooperative EHs on the achievable average sum secrecy rate for system parameters $N = 8$, $K = 3$, $M = 2$, $\bar{E} = 2\ mW$, $Pt = 1\ W$ and $\zeta = 0.5$. For that purpose, the statistical average of the channel power gains (channel variance) from the BS to all EHs are kept constant at $\gamma_E^2 = 10^{-3}$, therefore, the problem feasibility will not be affected, while channel variance from the BS to all IUs is varied over the range

---

[1]This is the lower bound on the optimal solution performance since the suboptimal solution performances still lie under this lower bound.
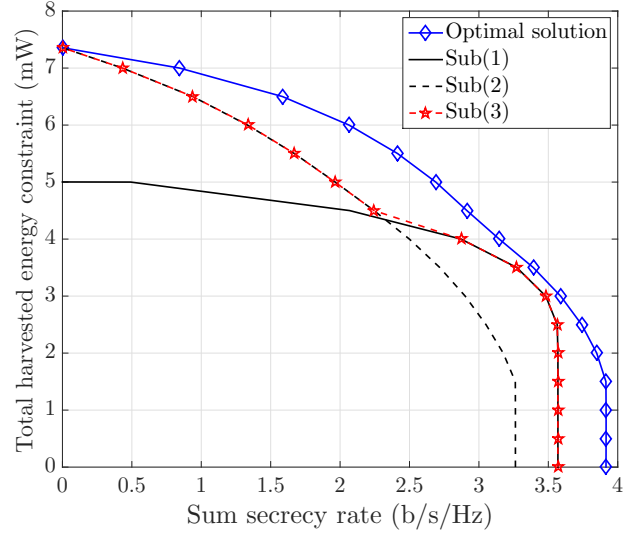

Fig. 3. E-R regions for cooperative EHs case with total harvested energy constraint.
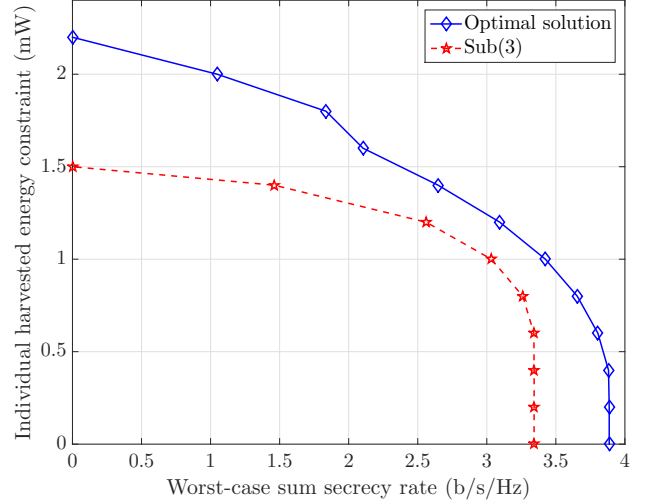

Fig. 4. E-R regions for the non-cooperative EHs case with individual harvested energy constraints.

$[-90\mathrm{dB}, -50\mathrm{dB}]$ which corresponds to channel variance range from $\gamma_I^2 = 10^{-9}$ to $\gamma_I^2 = 10^{-5}$. As expected, the average sum secrecy rate tends to decrease as the IUs signal attenuation increases.

Fig. 6 compares the average worst-case sum secrecy rate achieved by different optimization schemes against different number of transmit antennas at the BS with $K = 3$, $M = 2$, $\bar{E} = 3\ mW$, $P_t = 1\ W$ and $\zeta = 0.5$. The value of $\bar{E}$ is chosen such that the three solutions, the optimal, Sub(1) and Sub(2) get a reasonable feasibility rate. Note that to calculate the average sum secrecy rate, only the feasible solution cases are considered. As expected at lower value of harvested energy constraint ($\bar{E} = 3\ mW$), the suboptimal solution Sub(1) outperforms Sub(2). The priority in AN precoding in Sub(1) is to nullify the AN at the IUs and this is appropriate at low harvested energy constraint region. It can be seen that the gap
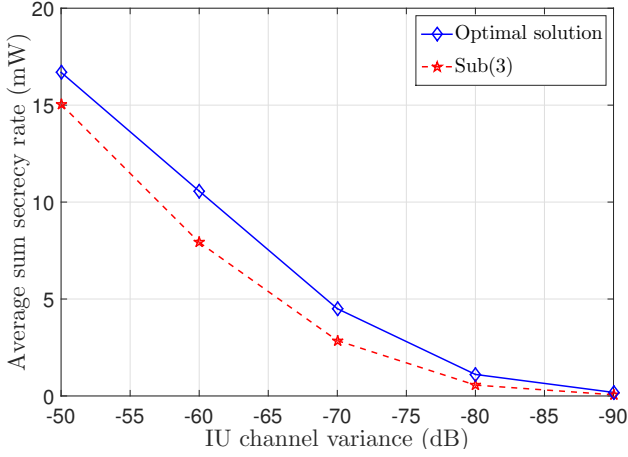
Fig. 5. Sum secrecy rate versus variance of IU channels with given harvested energy constraint $\bar{E} = 2 mW$.
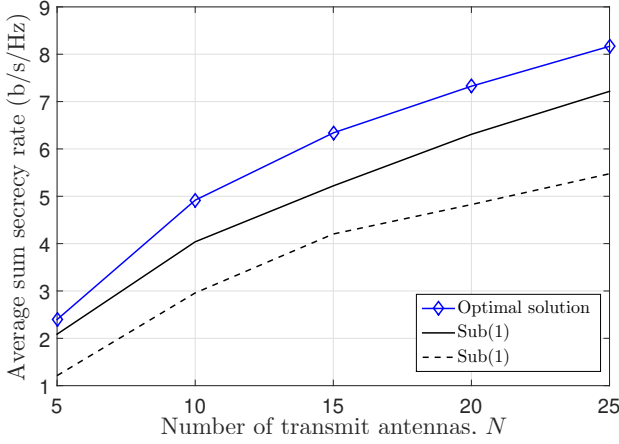

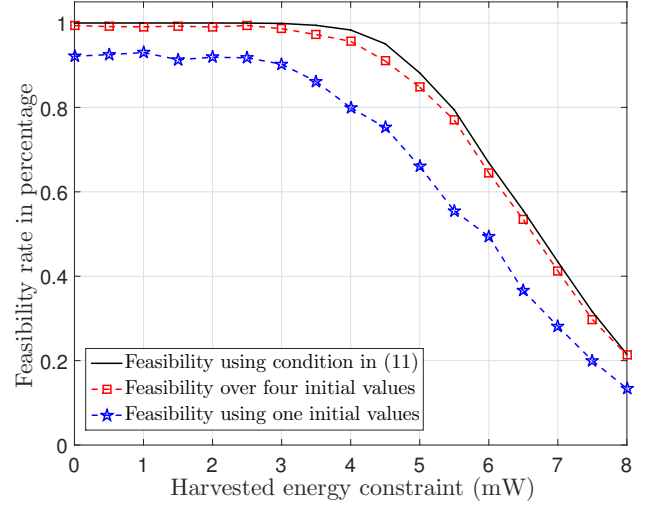Fig. 6. Achievable average sum secrecy rate for different numbers of transmit antennas.

Fig. 7. Optimal solution feasibility rate in percentage.

calculated as follows

$$\bar{v}_k = \log \left(\frac{P_t - P_n}{M} \sum_{i=1}^{M} \text{Tr} \left(\boldsymbol{G}_k \bar{\boldsymbol{w}}_m \bar{\boldsymbol{w}}_m^H \right) + \right.$$
$$\left. \frac{P_n}{2} \sum_{l=1}^{2} \text{Tr} \left(\boldsymbol{G}_k \bar{\boldsymbol{q}}_l \bar{\boldsymbol{q}}_l^H \right) + \sigma_E^2 \right), \ \forall i, \quad (49)$$

$$\bar{s}_i = \log \left(\frac{P_n}{2} \left| \boldsymbol{h}_i^H \bar{\boldsymbol{q}}_2 \right|^2 + \sigma_I^2 \right), \ \forall i, \quad (50)$$

where P_n is the total AN power. The values obtained by the above equations are based on the third suboptimal solution Sub(3), but with equal power allocation among the information beamforming vectors and the AN beamforming vectors. The initial values that yield a feasible first iteration (if it exists) is obtained via one-dimensional search across $0 \leq P_n \leq P_t$. The optimal solution feasibility rate in percentage is calculated using three different Monté-Carlo simulations. In the first two simulations, we inspect the actual optimization problem feasibility by solving problem (14) using CVX software. The initial values $\bar{s}$ and $\bar{v}$ are calculated by using (49) and (50) with a search through $P_n = 0, 0.2, 0.4, 0.6 \ W$ for the first simulation (square-marked curve), and for the second simulation results (star-marked curve), the initial values are calculated by (49) and (50) but only with $P_n = 0$. These two results are compared with problem feasibility rate obtained by the satisfaction of the condition in (11) (solid line curve). As we can see, searching through four different initial values of $\bar{s}$ and $\bar{v}$ yields a feasibility rate close to that obtained by feasibility condition (11), while when each of $\bar{s}$ and $\bar{v}$ are assigned one value, the feasibility rate drops significantly. This gives an insight into the sharpness of the feasibility condition (11).

Fig. 8 shows the achievable worst-case sum secrecy rate across the iterations of our iterative algorithms for both optimal solution and the sub-optimal solution, Sub(3). The results are obtained in the trade-off region of both solutions with a common total harvested energy constraint $\bar{E} = 5.5 \ mW$ and common initial values, $\bar{s}$ and $\bar{v}$, which are calculated by

between the average sum secrecy rate achieved by Sub(1) and Sub(2) increases with the number antennas. This is because, in Sub(1), as the number of transmit antennas increases, the percentage of channels used to match the AN signal toward the EHs increases with preserving the cancellation of the AN at the IUs. For example, at $N = 10$, equivalently, $80\% \left(\frac{10-2}{10} \times 100 \right)$ of the transmit antennas are used for AN alignment, whereas at $N = 25$, $92\% \left(\frac{25-2}{25} \times 100 \right)$ of the transmit antennas are used for AN alignment.

The feasibility of the optimal solution to problem (14) is mainly dependent on the parameters in the feasibility condition (11). In addition, the choice of the initial values of the slack variable vectors $\bar{s}$ and $\bar{v}$ can affect the feasibility of the first iteration. If the initial values of $\bar{s}$ and $\bar{v}$ are chosen far from the optimal values $\boldsymbol{s}^\star$ and $\boldsymbol{v}^\star$, then there is a strong possibility that the first iteration ends up infeasible or the solution takes a large number of iterations to converge. In Fig. 7, we examine the feasibility rate of the optimal solution in average percentage for a range of harvested energy constraint using the same simulation parameters in Fig. 2. A simple and good approximation for the initial values $\bar{s}$ and $\bar{v}$ are
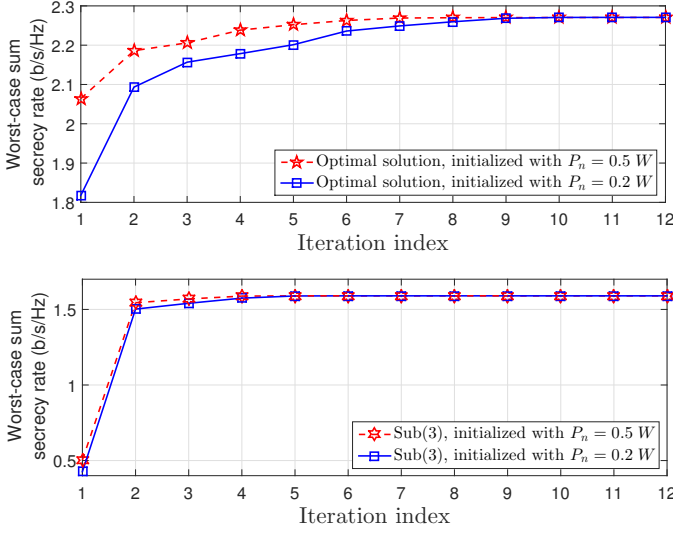
Fig. 8. Convergence of the achievable sum secrecy rate for the optimal and Sub(3) solutions, with non-cooperative EHs.

using (50) and (49) with $P_n = 0.2, 0.5\ W$. With a tolerance of $0.001\ b/s/Hz$, the optimal solution converges at the 10th and the 7th iterations with the initial values generated with $P_n = 0.2\ W$ and $P_n = 0.5\ W$, respectively. On the other hand, the sub-optimal solution converges at the 5th and the 4th iterations with the initial values generated with $P_n = 0.2\ W$ and $P_n = 0.5\ W$, respectively. The suboptimal solution shows a faster convergence speed than the optimal solution at different initial values. This is expected since the initial values are calculated by the beamforming vectors employed by the suboptimal solution.

IX. CONCLUSIONS

In this paper, we considered secure downlink transmission in SWIPT MU-MISO systems comprising multiple IUs and multiple EHs which have the potential to wire-tap the IU's signal. We proposed joint optimization of the information and AN beamforming vectors for worst-case sum secrecy rate maximization with a constraint on the total harvested energy by the EHs. The problem was formulated as an iterative SDP program. Using dual variable multipliers, we derived a rank-one solution for the transmit covariance matrices of the IUs which achieved the same optimal sum secrecy rate attained by a rank-unconstrained SDP program solution. Three different sub-optimal solutions were also provided. The first solution was based on IUs interference alignment and the projection of the AN in the null space of IUs channel vectors followed by transmission along the dominant eigenvector of the equivalent EHs channel, while the second solution ignored the AN alignment at the IUs. The third sub-optimal solution exploited the AN beamforming vectors of both the first and the second sub-optimal solutions. The performances of the sub-optimal solutions lied under the optimal solution, however, as a result of AN null space projection, the first sub-optimal solution outperformed the second solution in the low energy harvesting constraint region and vice versa for the high energy

harvesting constraint region. The sum secrecy rate achieved by the third sub-optimal solution traced the maximum of the first or the second sub-optimal solution. Future work will aim at optimizing transmit beamforming matrices for multi-antenna IUs and EHs, and also considering the work for the massive MU-MISO case.

APPENDIX
PROOF OF THEOREM I

Proof: For the SDR problems (14), the optimal rank-one solution $\widetilde{\mathbb{S}}^{\star_1}$ is obtained via two steps. In the first step, we find the structure of the optimal rank-unconstrained information beamforming matrices $\left\{\hat{\boldsymbol{W}}_m^{\star_1}\right\}$. Then, in the second step, we use the structure of $\left\{\hat{\boldsymbol{W}}_m^{\star_1}\right\}$ to calculate new optimal solution $\left\{\left\{\widetilde{\boldsymbol{W}}_m^{\star_1}\right\},\widetilde{\boldsymbol{Q}}^{\star_1},\widetilde{\boldsymbol{s}}^{\star_1},\widetilde{\boldsymbol{T}}^{\star_1},\boldsymbol{u}^{\star_1},\boldsymbol{v}^{\star_1}\right\} = \widetilde{\mathbb{S}}^{\star_1}$ that satisfies a rank-one constraint, $\text{rank}\left(\widetilde{\boldsymbol{W}}_{\bar{m}}^{\star_1}\right) = 1$, and achieves the same objective value achieved by $\left\{\left\{\hat{\boldsymbol{W}}_m^{\star_1}\right\},\hat{\boldsymbol{Q}}^{\star_1},\boldsymbol{s}^{\star_1},\boldsymbol{T}^{\star_1},\boldsymbol{u}^{\star_1},\boldsymbol{v}^{\star_1}\right\} = \mathbb{S}^{\star_1}$. The optimal rank-one solution of (15), $\widetilde{\mathbb{S}}^{\star_2}$, can be obtained by following the same steps, therefore, and due to space limitation, we provide the proof for (14) only.

Since the objective function and the constraints of (13) are differentiable, i. e., they have an open domain, then there is a solution set that can strictly satisfy the constraints (13a)-(13e). Therefore, Slater's condition holds, and zero gap between primal and dual solutions is guaranteed if the KKT conditions are satisfied [26]. The Lagrangian of problem (13) can be written as

$$\mathcal{L}\left(\mathbb{S},\mathbb{L}\right) = \sum_{i=1}^{M}\left(u_i - s_i - v_{k(i)} + t_{i,k(i)}\right) +$$
$$\sum_{i=1}^{M}\left(-\alpha_{3_i}e^{u_i} + \alpha_{4_i}e^{s_i} - \sum_{k=1}^{K}\alpha_{6_{i,k}}e^{t_{i,k}}\right) + \sum_{k=1}^{K}\alpha_{5_k}e^{v_k}$$
$$+ \sum_{m=1}^{M}\text{Tr}\left(\boldsymbol{A}_m\hat{\boldsymbol{W}}_m\right) + \text{Tr}\left(\boldsymbol{B}\hat{\boldsymbol{Q}}\right) + d, \qquad (51)$$

where

$$\boldsymbol{A}_m = -\alpha_1 + \zeta\alpha_2\hat{\boldsymbol{G}} + \sum_{i=1}^{M}\alpha_{3_i}\boldsymbol{H}_i - \sum_{k=1}^{K}\alpha_{5_k}\hat{\boldsymbol{G}}_k$$
$$+ \sum_{\substack{i=1\\i\neq m}}^{M}\left(-\alpha_{4_i}\boldsymbol{H}_i + \sum_{k=1}^{K}\alpha_{6_{i,k}}\hat{\boldsymbol{G}}_k\right) + \boldsymbol{Y}_m, \quad (52)$$

$$\boldsymbol{B} = -\alpha_1 + \zeta\alpha_2\hat{\boldsymbol{G}} - \sum_{k=1}^{K}\alpha_{5_k}\hat{\boldsymbol{G}}_k$$
$$+ \sum_{i=1}^{M}\left(\alpha_{3_i}\boldsymbol{H}_i - \alpha_{4_i}\boldsymbol{H}_i + \sum_{k=1}^{K}\alpha_{6_{i,k}}\hat{\boldsymbol{G}}_k\right) + \boldsymbol{Y}_Q,$$
$$(53)$$

$$d = \alpha_1 P_t - \alpha_2 \bar{E} + \sum_{i=1}^{M} \left((\alpha_{3_i} - \alpha_{4_i}) \sigma_I^2 + \sigma_E^2 \sum_{k=1}^{K} \alpha_{6_{i,k}} \right)$$
$$- \sigma_E^2 \sum_{k=1}^{K} \alpha_{5_k}, \tag{54}$$

and $\{\alpha_1, \alpha_2, \{\alpha_{3_i}\}, \{\alpha_{4_i}\}, \{\alpha_{5_k}\}, \{\alpha_{6_{i,k}}\}\} = \mathbb{L} \geq 0$ are the Lagrange multipliers associated with the constraints (8a), (8b), (13a), (13b), (13c) and (13d), respectively. The set $\{\boldsymbol{Y}_m\}, \boldsymbol{Y}_Q \succeq \boldsymbol{0}$ are the Lagrange multipliers associated with the semidefiniteness constraints in (8c), respectively, and $k(i) = \underset{k}{\operatorname{argmax}} (v_k - t_{i,k})$. Notice that, the Lagrange dual function $\mathcal{G}(\mathbb{L}, \{\boldsymbol{Y}_m\}, \boldsymbol{Y}_Q)$ is the supremum of $\mathcal{L}$ over $\mathbb{S}$. In order for $\mathcal{G}$ to exist, $\mathcal{G}$ has to be bounded from above, accordingly

$$\boldsymbol{A}_m, \boldsymbol{B} \preceq \boldsymbol{0}, \quad \{\alpha_{4_i}\}, \{\alpha_{5_k}\}, \{\alpha_{6_{i,k}} \mid k \neq k(i)\} = 0,$$
$$\text{and} \quad \{\alpha_{3_i}\}, \{\alpha_{6_{i,k(i)}}\} > 0. \tag{55}$$

Therefore, the Lagrangian function will be

$$\mathcal{G} = \alpha_1 P_t - \alpha_2 \bar{E} + \sum_{i=1}^{M} \left(\alpha_{3_i} \sigma_I^2 + \alpha_{6_{i,k(i)}} \sigma_E^2 \right)$$
$$+ \sum_{i=1}^{M} \left(\log \left(\frac{1}{\alpha_{3_i} \alpha_{6_{i,k(i)}}} \right) - 2 \right). \tag{56}$$

The primal problem (13) can be solved by solving the dual problem (57) which achieves the same objective value

$$\underset{\mathbb{L}, \{\boldsymbol{Y}_m\}, \boldsymbol{Y}_Q}{\text{Minimize}} \quad \mathcal{G}$$

subject to

$$\alpha_1, \alpha_2 \geq 0, \quad \{\alpha_{3_i}\}, \{\alpha_{6_{k(i)}}\} > 0, \{\boldsymbol{Y}_m\}, \boldsymbol{Y}_Q \succeq \boldsymbol{0}. \tag{57}$$

We prove that the KKT conditions for the relaxed primal variable $\{\hat{\boldsymbol{W}}_m\}$ are satisfied as follows:

1) Primal and Dual Feasibility: Based on the feasibility condition in (11) and the non-negativeness of dual variables, both primal and dual problems are feasible.

2) Complementary Slackness: Since Slater's condition holds, then

$$f(\mathbb{S}^{\star 1})$$
$$= \mathcal{G}\left(\mathbb{L}^{\star 1}, \{\boldsymbol{Y}_m^{\star 1}\}, \boldsymbol{Y}_Q^{\star 1}\right) = \sup_{\mathbb{S}} \mathcal{L}\left(\mathbb{S}, \mathbb{L}^{\star 1}, \{\boldsymbol{Y}_m^{\star 1}\}, \boldsymbol{Y}_Q^{\star 1}\right)$$
$$= \sup_{\mathbb{S}} \left[f(\mathbb{S}) + \alpha_1^{\star 1} h_1 + \alpha_2^{\star 1} h_2 + \sum_{i=1}^{M} \left(\alpha_{3_i}^{\star 1} h_{3_i} + \alpha_{4_i}^{\star 1} h_{4_i} + \right. \right.$$
$$\sum_{k=1}^{K} \alpha_{6_{i,k}}^{\star 1} h_{6_{i,k}} + \operatorname{Tr}\left(\boldsymbol{Y}_i^{\star 1} \hat{\boldsymbol{W}}_i\right) \right) + \sum_{k=1}^{K} \alpha_{5_k}^{\star 1} h_{5_k} +$$
$$\operatorname{Tr}\left(\boldsymbol{Y}_Q^{\star 1} \hat{\boldsymbol{Q}}\right) \Big]$$
$$\overset{(a)}{\geq} f(\mathbb{S}^{\star 1}) + \alpha_1^{\star 1} h_1^{\star 1} + \alpha_2^{\star 1} h_2^{\star 1} + \sum_{i=1}^{M} \left(\alpha_{3_i}^{\star 1} h_{3_i}^{\star 1} + \alpha_{4_i}^{\star 1} h_{4_i}^{\star 1} + \right.$$

$$\sum_{k=1}^{K} \alpha_{6_{i,k}}^{\star 1} h_{6_{i,k}}^{\star 1} + \operatorname{Tr}\left(\boldsymbol{Y}_i^{\star 1} \hat{\boldsymbol{W}}_i^{\star 1}\right) \right) + \sum_{k=1}^{K} \alpha_{5_k}^{\star 1} h_{5_k}^{\star 1} +$$
$$\operatorname{Tr}\left(\boldsymbol{Y}_Q^{\star 1} \hat{\boldsymbol{Q}}^{\star 1}\right)$$
$$\overset{(b)}{\geq} f(\mathbb{S}^{\star 1}), \tag{58}$$

where f is the primal objective function, $\left\{\mathbb{L}^{\star 1}, \{\boldsymbol{Y}_m^{\star 1}\}, \boldsymbol{Y}_Q^{\star 1}\right\}$ is the optimal solution of (57) and h_1, h_2, $\{h_{3_i}\}$, $\{h_{4_i}\}$, $\{h_{5_k}\}$ and $\{h_{6_{i,k}}\}$ are the left-hand side of the inequality constraints (8a), (8b) and (13a)-(13d) (after rewriting them as ≥ 0 inequalities), respectively. The inequality (a) follows since the supremum of the Lagrangian is greater than or equal to the value of the Lagrangian at any feasible set of $\{\mathbb{S}, \mathbb{L}^{\star 1}\}$ which includes $\{\mathbb{S}^{\star 1}, \mathbb{L}^{\star 1}\}$ [26]. The inequality (b) follows from the non-negativeness of the elements in $\alpha_1^{\star 1} h_1^{\star 1}$, $\alpha_2^{\star 1} h_2^{\star 1}$, $\{\alpha_{3_i}^{\star 1} h_{3_i}^{\star 1}\}$, $\{\alpha_{4_i}^{\star 1} h_{4_i}^{\star 1}\}$, $\{\alpha_{5_k}^{\star 1} h_{5_k}^{\star 1}\}$, $\left\{\alpha_{6_{i,k}}^{\star 1} h_{6_{i,k}}^{\star 1}\right\}$, $\left\{\operatorname{Tr}\left(\boldsymbol{Y}_i^{\star 1} \hat{\boldsymbol{W}}_i^{\star 1}\right)\right\}$, and $\operatorname{Tr}\left(\boldsymbol{Y}_Q^{\star 1} \hat{\boldsymbol{Q}}^{\star 1}\right)$. Therefore, the inequalities (a) and (b) hold only when each term in $\alpha_1^{\star 1} h_1^{\star 1}$, $\alpha_2^{\star 1} h_2^{\star 1}$, $\{\alpha_{3_i}^{\star 1} h_{3_i}^{\star 1}\}$, $\{\alpha_{4_i}^{\star 1} h_{4_i}^{\star 1}\}$, $\{\alpha_{5_k}^{\star 1} h_{5_k}^{\star 1}\}$, $\left\{\alpha_{6_{i,k}}^{\star 1} h_{6_{i,k}}^{\star 1}\right\}$, $\left\{\operatorname{Tr}\left(\boldsymbol{Y}_i^{\star 1} \hat{\boldsymbol{W}}_i^{\star 1}\right)\right\}$, and $\operatorname{Tr}\left(\boldsymbol{Y}_Q^{\star 1} \hat{\boldsymbol{Q}}^{\star 1}\right)$ is equal to zero. Hence, the complimentary slackness is proved.

3) Stationarity: The stationary point of $\mathcal{L}$ should satisfy

$$\sum_{m=1}^{M} \frac{\partial \mathcal{L}}{\partial \hat{\boldsymbol{W}}_m^{\star 1}} = \boldsymbol{0}, \quad \text{therefore} \quad \sum_{m=1}^{M} \boldsymbol{A}_m^{\star 1} = \boldsymbol{0}.$$

Since we have $\boldsymbol{A}_m^{\star 1} \preceq \boldsymbol{0}$, $\forall m$, then, based on stationarity, (52) and (55), we have

$$\boldsymbol{Y}_m^{\star 1} = \boldsymbol{D}_m^{\star 1} - \sum_{i=1}^{M} \alpha_{3_i}^{\star 1} \boldsymbol{H}_i, \ \forall m, \tag{59}$$

$$\boldsymbol{D}_m^{\star 1} = \alpha_1^{\star 1} - \zeta \alpha_2^{\star 1} \hat{\boldsymbol{G}} - \sum_{\substack{i=1 \\ i \neq m}}^{M} \alpha_{6_{i,k(i)}}^{\star 1} \hat{\boldsymbol{G}}_{k(i)}. \tag{60}$$

To satisfy the complementary slackness condition, $\boldsymbol{W}_m^{\star 1}$ should lie in the null space of $\boldsymbol{Y}_m^{\star 1}$. Define $\operatorname{rank}\left(\boldsymbol{Y}_m^{\star 1}\right) = r_{1_m}$, $\operatorname{rank}\left(\boldsymbol{D}_m^{\star 1}\right) = r_{2_m}$, $\operatorname{null}\left(\boldsymbol{Y}_m^{\star 1}\right) = \boldsymbol{\Omega}_m \in \mathbb{C}^{N \times (N - r_{1_m})}$ and $\operatorname{null}\left(\boldsymbol{D}_m^{\star 1}\right) = \boldsymbol{\Psi}_m = \left[\boldsymbol{\psi}_{m,1}, ..., \boldsymbol{\psi}_{m, N - r_{2_m}}\right] \in \mathbb{C}^{N \times (N - r_{2_m})}$. Let $\boldsymbol{\psi}_{m,n}$ be the nth column of $\boldsymbol{\Psi}_m$. Then we have

$$\boldsymbol{\psi}_{m,n}^H \boldsymbol{Y}_m^{\star 1} \boldsymbol{\psi}_{m,n} = \boldsymbol{\psi}_{m,n}^H \left(\boldsymbol{D}_m^{\star 1} - \sum_{i=1}^{M} \alpha_{3_i}^{\star 1} \boldsymbol{H}_i\right) \boldsymbol{\psi}_{m,n} =$$
$$- \boldsymbol{\psi}_{m,n}^H \left(\sum_{i=1}^{M} \alpha_{3_i}^{\star 1} \boldsymbol{H}_i\right) \boldsymbol{\psi}_{m,n} = - \sum_{i=1}^{M} \alpha_{3_i}^{\star 1} \left| \boldsymbol{h}_i^H \boldsymbol{\psi}_{m,n} \right|^2. \tag{61}$$

Since $\boldsymbol{Y}_m^{\star 1} \succeq 0$, $\boldsymbol{H}_i \succeq 0$ and $\{\alpha_{3_i}^{\star 1}\} > 0$, hence

$$\left(\sum_{i=1}^{M} \alpha_{3_i}^{\star 1} \boldsymbol{H}_i\right) \boldsymbol{\Psi}_m = \boldsymbol{0}. \tag{62}$$

Accordingly, the column vectors in $\boldsymbol{\Psi}_m$ are in the null space of $\boldsymbol{Y}_m^{\star_1}$, therefore, $\boldsymbol{\Psi}_m$ is a sub-matrix of $\boldsymbol{\Omega}_m$ and the inequality $\operatorname{rank}(\boldsymbol{\Psi}_m) \leq \operatorname{rank}(\boldsymbol{\Omega}_m)$ is always true.

The $N \times N$ positive semidefinite matrix $\boldsymbol{Y}_m^{\star_1}$ satisfies the following

$$\operatorname{rank}(\boldsymbol{\Omega}_m) = N - \operatorname{rank}\left(\boldsymbol{Y}_m^{\star_1}\right). \tag{63}$$

Since $\left\{\alpha_{3_i}^{\star_1}\right\} > 0$, and $\{\boldsymbol{H}_i\} \succeq \boldsymbol{0}$ are statistically independent rank-one matrices, then $\sum_{i=1}^{M} \alpha_{3_i}^{\star_1} \boldsymbol{H}_i$ is a positive semidefinite matrix of a rank $\leq M$ (most likely equal to M). Therefore, by applying the result of *Lemma A.1* in [6] to (59), we have, $\operatorname{rank}\left(\boldsymbol{Y}_m^{\star_1}\right) \geq \operatorname{rank}\left(\boldsymbol{D}_m^{\star_1}\right) - M$. Substituting this inequality in (63) results in

$$\begin{aligned}
\operatorname{rank}(\boldsymbol{\Omega}_m) &\leq N - \operatorname{rank}\left(\boldsymbol{D}_m^{\star_1}\right) + M \\
&\leq \operatorname{rank}(\boldsymbol{\Psi}_m) + M.
\end{aligned} \tag{64}$$

Therefore,

$$\operatorname{rank}(\boldsymbol{\Psi}_m) \leq \operatorname{rank}(\boldsymbol{\Omega}_m) \leq \operatorname{rank}(\boldsymbol{\Psi}_m) + M. \tag{65}$$

Now, let us consider the case, $\operatorname{rank}(\boldsymbol{\Omega}_m) = \operatorname{rank}(\boldsymbol{\Psi}_m)$, i.e., $\boldsymbol{\Omega}_m = \boldsymbol{\Psi}_m$ and $\boldsymbol{W}_m^{\star_1} = a_{m,n} \boldsymbol{\psi}_{m,n} \boldsymbol{\psi}_{m,n}^H$, $a_{m,n} > 0$. This solution can not be optimal since it leads to a negative secrecy rate at the IU_m along with inter-user interference, moreover, the noise imposed by $\boldsymbol{W}_m^{\star_1}$ on the EHs can be attained by the AN beamformers $\boldsymbol{q}_l$s which are statistically independent, and therefore, $\boldsymbol{W}_m^{\star_1} = \boldsymbol{0}$ will definitely perform better. As a result, the case $\operatorname{rank}(\boldsymbol{\Omega}_m) = \operatorname{rank}(\boldsymbol{\Psi}_m)$ does not exist and there are always between 1 and M unit norm vector(s) $\left[\boldsymbol{\omega}_{m,1}, ..., \boldsymbol{\omega}_{m,r_{2_m}-r_{1_m}}\right]$ which satisfy $\boldsymbol{\Omega}_m = \left[\boldsymbol{\Psi}_m \left[\boldsymbol{\omega}_{m,1}, ..., \boldsymbol{\omega}_{m,r_{2_m}-r_{1_m}}\right]\right]$. Then, we can write the optimal solution for $\hat{\boldsymbol{W}}_m^{\star_1} \in \left\{\hat{\boldsymbol{W}}_{\bar{m}}^{\star_1}\right\}$ as

$$\sum_{n=1}^{N-r_{2_m}} a_{m,n} \boldsymbol{\psi}_{m,n} \boldsymbol{\psi}_{m,n}^H + \sum_{n_1=1}^{r_{2_m}-r_{1_m}} b_{m,n_1} \boldsymbol{\omega}_{m,n_1} \boldsymbol{\omega}_{m,n_1}^H, \tag{66}$$

where $b_{m,n1}$s > 0 are positive scaling constants.

In the following, we can construct a non-unique optimal solution $\widetilde{\mathbb{S}}^{\star_1}$ that satisfies $\operatorname{rank}\left(\widetilde{\boldsymbol{W}}_m^{\star_1}\right) = 1$ and can achieve the same objective value achieved by $\hat{\boldsymbol{W}}_m^{\star_1}$ as follows

$$\widetilde{\boldsymbol{W}}_m^{\star_1} = b_{m,\bar{n}_{1_m}} \boldsymbol{\omega}_{m,\bar{n}_m} \boldsymbol{\omega}_{m,\bar{n}_m}^H = \begin{cases} \hat{\boldsymbol{W}}_m^{\star_1} - \boldsymbol{\tau}_m & \forall m \in \{\bar{m}\} \\ \hat{\boldsymbol{W}}_m^{\star_1}, & \forall m \notin \{\bar{m}\} \end{cases}, \tag{67}$$

$$\widetilde{s}_m^{\star_1} = \\
\begin{cases} s_m^{\star_1} + \delta_m^{(1)}, & \forall m \in \{\bar{m}\}, \operatorname{Tr}(\boldsymbol{H}_m \boldsymbol{\tau}_m) \leq \operatorname{Tr}(\boldsymbol{G}_{k(m)} \boldsymbol{\tau}_m) \\ s_m^{\star_1} + \delta_m^{(2)}, & \forall m \in \{\bar{m}\}, \operatorname{Tr}(\boldsymbol{H}_m \boldsymbol{\tau}_m) \geq \operatorname{Tr}(\boldsymbol{G}_{k(m)} \boldsymbol{\tau}_m) \\ s_m^{\star_1}, & \forall m \notin \{\bar{m}\}, \end{cases} \tag{68}$$

$$\widetilde{t}_{m,k(m)}^{\star_1} =$$

$$\begin{cases} t_{m,k(m)}^{\star_1} + \delta_m^{(1)}, & \forall m \in \{\bar{m}\}, \operatorname{Tr}(\boldsymbol{H}_m \boldsymbol{\tau}_m) \leq \operatorname{Tr}(\boldsymbol{G}_{k(m)} \boldsymbol{\tau}_m) \\ t_{m,k(m)}^{\star_1} + \delta_m^{(2)}, & \forall m \in \{\bar{m}\}, \operatorname{Tr}(\boldsymbol{H}_m \boldsymbol{\tau}_m) \geq \operatorname{Tr}(\boldsymbol{G}_{k(m)} \boldsymbol{\tau}_m) \\ t_{m,k(m)}^{\star_1}, & \forall m \notin \{\bar{m}\}, \end{cases} \tag{69}$$

and

$$\widetilde{\boldsymbol{Q}}^{\star_1} = \hat{\boldsymbol{Q}}^{\star_1} + \sum_{m \in \{\bar{m}\}} \boldsymbol{\tau}_m, \tag{70}$$

where

$$\bar{n}_m \in \{1, ..., r_{2_m} - r_{1_m}\}, \tag{71}$$

$$\boldsymbol{\tau}_m = \sum_{n=1}^{N-r_{2_m}} a_{m,n} \boldsymbol{\psi}_{m,n} \boldsymbol{\psi}_{m,n}^H + \sum_{\substack{n_1=1 \\ n_1 \neq \bar{n}_{1_m}}}^{N-r_m} b_{m,n_1} \boldsymbol{\omega}_{m,n_1} \boldsymbol{\omega}_{m,n_1}^H, \tag{72}$$

$$\delta_m^{(1)} = -s_m^{\star_1} + \log\left(\operatorname{Tr}(\boldsymbol{H}_m \boldsymbol{\tau}_m) + e^{s_m^{\star}}\right), \tag{73}$$

$$\delta_m^{(2)} = -t_{m,k(m)}^{\star_1} + \log\left(\operatorname{Tr}(\boldsymbol{G}_{k(m)} \boldsymbol{\tau}_m) + e^{t_{m,k(m)}^{\star}}\right). \tag{74}$$

By substituting $\widetilde{\mathbb{S}}^{\star_1}$ into the constraints and the objective function of problem (13), it can be verified that $\widetilde{\mathbb{S}}^{\star_1}$ satisfies all the constraints (13a)-(13e) and achieves the same sum secrecy rate as $\mathbb{S}^{\star_1}$ does. This concludes the proof. ∎

REFERENCES

[1] N. Tesla, "Apparatus for transmitting electrical energy." Dec. 1 1914, US Patent 1,119,732.

[2] S. Y. R. Hui, W. Zhong, and C. K. Lee, "A critical review of recent progress in mid-range wireless power transfer," *IEEE Trans. Power Electron.*, vol. 29, no. 9, pp. 4500–4511, Sep. 2014.

[3] C. K. Lee, W. Zhong, and S. Y. R. Hui, "Recent progress in mid-range wireless power transfer," in *Energy Conversion Congress and Exposition (ECCE), 2012 IEEE.* IEEE, Sep. 2012, pp. 3819–3824.

[4] T. Imura and Y. Hori, "Maximizing air gap and efficiency of magnetic resonant coupling for wireless power transfer using equivalent circuit and Neumann formula," *IEEE Trans. Ind. Electron.*, vol. 58, no. 10, pp. 4746–4752, Oct. 2011.

[5] S. Jung, S. Jeong, and J. Kang, "Joint transceiver design for secure communication with power transfer," in *Annual International Symposium on Personal, Indoor, and Mobile Radio Communication (PIMRC).* IEEE, Sep. 2014, pp. 37–41.

[6] L. Liu, R. Zhang, and K.-C. Chua, "Secrecy wireless information and power transfer with MISO beamforming," *IEEE Trans. Signal Process.*, vol. 62, no. 7, pp. 1850–1863, Jan. 2014.

[7] D. W. K. Ng, E. S. Lo, and R. Schober, "Robust beamforming for secure communication in systems with wireless information and power transfer," *IEEE Trans. Wireless Commun.*, vol. 13, no. 8, pp. 4599–4615, Apr. 2014.

[8] M. R. Khandaker and K.-K. Wong, "Masked beamforming in the presence of energy-harvesting eavesdroppers," *IEEE Transactions on Information Forensics and Security*, vol. 10, no. 1, pp. 40–54, Oct. 2015.

[9] H. Zhang, C. Li, Y. Huang, and L. Yang, "Secure beamforming for SWIPT in multiuser MISO broadcast channel with confidential messages," *IEEE Commun. Lett.*, vol. 19, no. 8, pp. 1347–1350, Jun. 2015.

[10] M. Zhang, K. Cumanan, and A. Burr, "Secrecy rate maximization for MISO multicasting SWIPT system with power splitting scheme," *arXiv preprint arXiv:1605.02055*, Jul. 2016.

[11] J. Park and B. Clerckx, "Joint wireless information and energy transfer in a two-user MIMO interference channel," *IEEE Trans. Wireless Commun.*, vol. 12, no. 8, pp. 4210–4221, Aug. 2013.

[12] Q. Zhang, X. Huang, Q. Li, and J. Qin, "Cooperative jamming aided robust secure transmission for wireless information and power transfer in MISO channels," *IEEE Trans. Commun.*, vol. 63, no. 3, pp. 906–915, Feb. 2015.

[13] S. Jeong, K. Lee, H. Huh, and J. Kang, "Secure transmission in downlink cellular network with a cooperative jammer," *IEEE Commun. Lett.*, vol. 2, no. 4, pp. 463–466, Jun. 2013.

[14] A. El Shafie, D. Niyato, and N. Al-Dhahir, "Artificial-noise-aided secure mimo full-duplex relay channels with fixed-power transmissions," *IEEE Commun. Lett.*, vol. 20, no. 8, pp. 1591–1594, Jun. 2016.

[15] L. Hu, B. Wu, J. Tang, F. Pan, and H. Wen, "Outage constrained secrecy rate maximization using artificial-noise aided beamforming and cooperative jamming," in *IEEE International Conference on Communications (ICC)*. IEEE, May 2016, pp. 1–5.

[16] N. Sklavos and X. Zhang, *Wireless security and cryptography: specifications and implementations*. CRC Press, 2007.

[17] P. A. Regalia, A. Khisti, Y. Liang, and S. Tomasin, "Secure communications via physical-layer and information-theoretic techniques [scanning the issue]," *Proc. IEEE*, vol. 103, no. 10, pp. 1698–1701, Oct. 2015.

[18] A. Sayeed and A. Perrig, "Secure wireless communications: Secret keys through multipath," in *2008 IEEE International Conference on Acoustics, Speech and Signal Processing*. IEEE, Mar. 2008, pp. 3013–3016.

[19] M. Zafer, D. Agrawal, and M. Srivatsa, "Limitations of generating a secret key using wireless fading under active adversary," *IEEE/ACM Transactions on Networking (TON)*, vol. 20, no. 5, pp. 1440–1451, Oct. 2012.

[20] K. Zeng, D. Wu, A. Chan, and P. Mohapatra, "Exploiting multiple-antenna diversity for shared secret key generation in wireless networks," in *INFOCOM, Proceedings IEEE*. IEEE, Mar. 2010, pp. 1–9.

[21] S. Liu, Y. Hong, and E. Viterbo, "Unshared secret key cryptography," *IEEE Transactions on Wireless Communications*, vol. 13, no. 12, pp. 6670–6683, Dec. 2014.

[22] M. Zhang and Y. Liu, "Energy harvesting for physical-layer security in OFDMA networks," *IEEE Trans. Inf. Forensics Security*, vol. 11, no. 1, pp. 154–162, Sep. 2016.

[23] K. Huang and E. Larsson, "Simultaneous information and power transfer for broadband wireless systems," *IEEE Trans. Signal Process.*, vol. 61, no. 23, pp. 5972–5986, Sep. 2013.

[24] M. Zhang, Y. Liu, and R. Zhang, "Artificial noise aided secrecy information and power transfer in OFDMA systems," *IEEE Trans. Wireless Commun.*, vol. 15, no. 4, pp. 3085–3096, Jan. 2016.

[25] ——, "Secrecy wireless information and power transfer in OFDMA systems," in *IEEE Global Communications Conference (GLOBECOM)*. IEEE, Dec. 2015, pp. 1–6.

[26] S. Boyd and L. Vandenberghe, *Convex optimization*. Cambridge University Press, 2004.

[27] F. Zhang and Q. Zhang, "Eigenvalue inequalities for matrix product," *IEEE Trans. Autom. Control*, vol. 51, no. 9, p. 1506, Sep. 2006.

[28] P. Zhao, M. Zhang, H. Yu, H. Luo, and W. Chen, "Robust beamforming design for sum secrecy rate optimization in MU-MISO networks," *IEEE Trans. Inf. Forensics Security*, vol. 10, no. 9, pp. 1812–1823, Apr. 2015.

[29] M. Grant and S. Boyd, "CVX: Matlab software for disciplined convex programming, version 1.21, Apr. 2011," *Available: cvxr. com/cvx*.

[30] M. Razaviyayn, "Successive convex approximation: Analysis and applications," Ph.D. dissertation, Ph.D. dissertation, UNIVERSITY OF MINNESOTA, 2014.

[31] R. Tütüncü, K. Toh, and M. Todd, "SDPT3—a Matlab software package for semidefinite-quadratic-linear programming, version 3.0," *Web page http://www. math. nus. edu. sg/~ mattohkc/sdpt3. html*, Aug. 2001.

[32] A. Ben-Tal and A. Nemirovski, *Lectures on modern convex optimization: analysis, algorithms, and engineering applications*. SIAM, Jan. 2001.

[33] M. X. Goemans and D. Williamson, "Approximation algorithms for MAX–3–CUT and other problems via complex semidefinite programming," in *Proceedings of the thirty-third annual ACM symposium on Theory of computing*. ACM, Jul. 2001, pp. 443–452.

[34] D. Tse and P. Viswanath, *Fundamentals of wireless communication*. Cambridge University Press, May 2005.

[35] M. Hata, "Empirical formula for propagation loss in land mobile radio services," *IEEE Trans. Veh. Technol.*, vol. 29, no. 3, pp. 317–325, Aug. 1980.

[36] T. Le, K. Mayaram, and T. Fiez, "Efficient far-field radio frequency energy harvesting for passively powered sensor networks," *IEEE J. Solid-State Circuits*, vol. 43, no. 5, pp. 1287–1302, May 2008.

Mahmoud Alageli received the B.Sc. degree in Electrical and Electronic Engineering from the Engineering Academy Tajoura, Tripoli, Libya, in 1999. He then received the M.Eng. degree in Communication and Computer from National University of Malaysia, Malaysia, in 2006. He is currently pursuing the Ph.D. degree with the Intelligent Sensing and Communications group at Newcastle University, Newcastle upon Tyne, UK. His current research interests include energy harvesting communications, physical layer security and massive MIMO.

Aissa Ikhlef (M'09) was born in Constantine, Algeria. He received the B.S. degree in Electrical Engineering from the University of Constantine, Constantine, Algeria, in 2001 and the M.Sc. and Ph.D. degrees in Electrical Engineering from the University of Rennes 1, Rennes, France, in 2004 and 2008, respectively. From 2004 to 2008, he was with Supélec, France, pursuing his Ph.D. degree. From 2007 to 2008, he was a Lecturer at the University of Rennes 1. From 2008 to 2010 he was a Postdoctoral Fellow with the Communication and Remote Sensing Laboratory, Catholic University of Louvain, Louvain La Neuve, Belgium. He was a visiting Postdoctoral Fellow at the University of British Columbia, Vancouver, BC, Canada, from August to November 2009. From 2010 to 2013 he was with the data communications group, University of British Columbia, Vancouver, Canada, as a Postdoctoral Fellow. From June 2013 to August 2014 he was with Toshiba Research Europe Limited, Bristol, UK, as a Senior Research Engineer. From September 2014 to August 2016 he was with the School of Electrical and Electronic Engineering, Newcastle University, Newcastle, UK, as a Lecturer (Assistant Professor). Since September 2016 he has been an Assistant Professor with the School of Engineering and Computing Sciences, Durham University, Durham, UK. He served as an Editor for IEEE Communications Letters from 2014 to 2016. His current research interests include energy harvesting communications, physical layer security, and massive MIMO.

Jonathon Chambers (S'83–M'90–SM'98–F'11) received the Ph.D. and D.Sc. degrees in signal processing from the Imperial College of Science, Technology and Medicine (Imperial College London), London, U.K., in 1990 and 2014, respectively. From 1991 to 1994, he was a Research Scientist with the Schlumberger Cambridge Research Center, Cambridge, U.K. In 1994, he returned to Imperial College London as a Lecturer in signal processing and was promoted to Reader (Associate Professor) in 1998. From 2001 to 2004, he was the Director of the Center for Digital Signal Processing and a Professor of signal processing with the Division of Engineering, King's College London and is now a Visiting Professor. From 2004 to 2007, he was a Cardiff Professorial Research Fellow with the School of Engineering, Cardiff University, Cardiff, U.K. Between 2007–2014, he led the Advanced Signal Processing Group, within the School of Electronic, Electrical and Systems Engineering, Loughborough University, and is now a Visiting Professor. In 2015, he joined the School of Electrical and Electronic Engineering, from the 1st Aug 2017 the School of Engineering, Newcastle University, where he is a Professor of signal and information processing and heads the Intelligent Sensing and Communications group. He is also an International Honorary Dean and Guest Professor within the Department of Automation at Harbin Engineering University, China. He has advised almost 80 researchers through to Ph.D. graduation and published more than 500 conference proceedings and journal articles, many of which are in IEEE journals. His research interests include adaptive signal processing and machine learning and their application in communications, defence and navigation systems.

Dr. Chambers is a Fellow of the Royal Academy of Engineering, U.K., the Institution of Engineering and Technology, and the Institute of Mathematics and its Applications. He was a Technical Program Co-chair for the 36th IEEE International Conference on Acoustics, Speech, and Signal Processing (ICASSP), Prague, Czech Republic and is serving on the organising committees of ICASSP 2019 Brighton, UK, and ICASSP 2022, Singapore. He has served on the IEEE Signal Processing Theory and Methods Technical Committee for six years, the IEEE Signal Processing Society Awards Board for three years, and the Jack Kilby Medal Commitee for three years.